ACADÉMIE
DES SCIENCES
INSTITUT DE FRANCE

Comptes Rendus

Géoscience

Sciences de la Planète

Marine A. Denolle, Qibin Shi, Tim Clements, Loïc Viens,
Veronica Rodriguez-Tribaldos and Fabrice Cotton

Ambient field seismology in critical zone hydrological sciences

Volume 357 (2025), p. 425-451

Online since: 6 October 2025

https://doi.org/10.5802/crgeos.310

The Comptes Rendus. Géoscience — Sciences de la Planète *are a member of the Mersenne Center for open scientific publishing*
www.centre-mersenne.org — e-ISSN : 1778-7025

ACADÉMIE DES SCIENCES
INSTITUT DE FRANCE

Comptes Rendus. Géoscience — Sciences de la Planète
2025, Vol. 357, p. 425-451
https://doi.org/10.5802/crgeos.310

Review article
Critical zone and socio-ecosystems

Ambient field seismology in critical zone hydrological sciences

Marine A. Denolle [*,a], **Qibin Shi** [a], **Tim Clements** [b], **Loïc Viens** [c], **Veronica Rodriguez-Tribaldos** [d] **and Fabrice Cotton** [d]

[a] Department of Earth and Space Sciences, University of Washington, Seattle, WA, USA

[b] United States Geological Survey, 350 N. Akron Rd. Moffett Field, CA 94035, USA

[c] Los Alamos National Laboratory, P.O. Box 1663 Los Alamos, NM 87545, USA

[d] GFZ Helmholtz Centre for Geosciences, Telegrafenberg 14473 Potsdam, Germany

E-mails: mdenolle@uw.edu (M. Denolle), qibins@uw.edu (Q. Shi), tclements@usgs.gov (T. Clements), lviens@lanl.gov (L. Viens), verort@gfz-potsdam.de (V. Rodriguez-Tribaldos), fcotton@gfz-potsdam.de (F. Cotton)

Abstract. Passive ambient noise monitoring is an emerging tool in environmental seismology, leveraging the ambient seismic field to assess temporal variations in shallow subsurface properties. This review focuses on the potential and challenges of using scattered coda waves from noise correlation functions to monitor critical zone dynamics. The sensitivity of seismic velocities to various environmental factors, including precipitation, snowmelt, atmospheric pressure, and groundwater fluctuations, underscores the method's versatility. While coda waves excel in detecting subtle changes due to their scattered nature, ballistic waves provide higher spatial resolution, albeit with challenges in source stability. Advances in seismic sensing, including distributed acoustic sensing and low-cost geophone networks, have enabled high-resolution monitoring of hydrological processes, subsurface deformation, and seismic hazards. Integrating seismic data with hydrological models provides insights into water storage, pore pressure changes, and soil moisture dynamics. However, limitations in spatial resolution, calibration with ground truth data, and coupled effects between environmental factors remain key challenges. This review emphasizes the importance of interdisciplinary approaches in refining methodologies, enhancing sensor deployments, and addressing data gaps. Passive seismic monitoring offers opportunities to understand critical zone processes and their broader impacts on seismic hazards and environmental sustainability.

Keywords. Critical zone, Environmental seismology, Ambient noise monitoring.

Funding. David and Lucile Packard Foundation, LA-UR-25-20095 by Triad National Security, LLC, U.S. Department of Energy (no. 89233218CNA000001), Los Alamos National Laboratory Center for Space and Earth Science Chick Keller Fellowship, USGS Mendenhall fellowship, National Science Foundation's Seismological Facility for the Advancement of Geoscience (SAGE) Award under Cooperative Agreement EAR-1724509.

Manuscript received 6 January 2025, revised 10 September 2025, accepted 18 August 2025.

[*] Corresponding author

1. Introduction

1.1. *Broad overview*

The Critical Zone (CZ) is Earth's near-surface region where freshwater, air, soil, rock, and living organisms interact, extending from the vegetation canopy at the surface down to freely circulating groundwater stored in aquifers (Giardino and Houser, 2015). Monitoring soil moisture in the CZ and understanding its dynamics is critical to improving agricultural management, monitoring droughts, floods, and groundwater recharge, and monitoring the stability of slope failures, and thus has implications for food security, climate systems, and surface hazards (floods, landslides, and earthquake-induced liquefaction). The spatial heterogeneity of soils' properties (e.g., hydraulic conductivity) and their potential for evapotranspiration, geological structure, meteorological forcing (e.g., precipitation, wind, and radiation), and vegetation control the spatial heterogeneity of soil moisture (e.g., Chaney et al., 2015). Conventional soil moisture monitoring is through (1) in situ soil moisture probes (Su et al., 2014) that have local sensitivity or (2) remote or airborne data that use electromagnetic wave signals (amplitudes and phase) to estimate soil moisture and have regional or global sensitivity (Babaeian et al., 2019). As stated by Flinchum, Holbrook, et al. (2022), "a major challenge in CZ science is to obtain measurements that have both high spatial resolution and cover large areas".

Passive ambient noise monitoring refers to the methodology of using repeated cross-correlation of the ambient seismic field, recorded at a single or a pair of seismic stations, to estimate the changes in seismic properties in the subsurface. We focus this review on the scattered waves in the coda of coherent ambient seismic waves, which are typically surface waves in the context of soils and sediments. "Ambient noise monitoring" is transforming environmental seismology as it provides new passive methods to monitor the mechanical response of the shallow subsurface (e.g., Larose et al., 2015; Le Breton et al., 2021; Q.-Y. Wang and Yao, 2020). Temporal variations in near-surface seismic properties stem from a range of interacting factors whose relative importance is frequently site-dependent, underscoring the spatial heterogeneity of soils. This review sets out to build a unified framework for monitoring hydromechanical behavior in the critical zone with ambient-noise seismology, examining the method's strengths and limitations.

Relative changes in shallow seismic velocities, $\mathrm{d}v/v$ hereafter, have been observed to vary between 0.1% and 50% under many tectonic and volcanic factors (e.g., Wegler and Sens-Schönfelder, 2007; Brenguier, Campillo, et al., 2008; Brenguier, Shapiro, et al., 2008; Obermann, Froment, et al., 2014; Yukutake et al., 2016; Feng, Huang and Wu, 2020; Cabrera-Pérez et al., 2023; Donaldson et al., 2019; Okubo et al., 2024; Esfahani et al., 2024) and solid Earth tides (e.g., Sens-Schönfelder and Eulenfeld, 2019; Mao, Campillo, et al., 2019; Takano and Nishida, 2023; Kramer, Y. Lu and Bokelmann, 2023). In addition to the rise in analyses monitoring temporal changes in the subsurface induced by earthquakes or volcanic activity, there are numerous environmental factors that change seismic properties of the subsurface: varying snow load (Q.-Y. Wang, Brenguier, et al., 2017; Donaldson et al., 2019), rainfall load and diffusion (Q.-Y. Wang, Brenguier, et al., 2017; Andajani et al., 2020; Feng, Huang, Hsu, et al., 2021; Clements and Denolle, 2023), atmospheric pressure fluctuations (Gradon et al., 2021; Kramer, Y. Lu and Bokelmann, 2023; Kramer, Y. Lu, Q.-Y. Wang, et al., 2025), river and lake levels (e.g., Rodríguez Tribaldos and Ajo-Franklin, 2021), thawing and freezing of soils (e.g., James, Knox, Abbott, Panning, et al., 2019). Figure 1 represents the vast range of time and spatial scales at which the hydrological phenomena have been reported to carry seismic signatures in the literature reviewed in this manuscript.

The core principle of ambient noise monitoring is that repeated measurements of the seismic wavefield, measured through the cross-correlation of the ambient seismic field between channels and stations, capture the seismic signatures of changes in effective stress or pore pressure. Coda waves extracted from "noise correlation functions" (NCFs) are commonly used in ambient noise monitoring, as they are less affected by variations in noise sources than direct waves (e.g., Hadziioannou, Larose, Coutant, et al., 2009; Colombi et al., 2014). Recently, using the direct, or ballistic, waves of the NCF, typically either P-waves or surface waves (e.g., Garambois et al., 2019; Takano, Brenguier, et al., 2019; Mordret et al., 2020; Brenguier, Courbis, et al., 2020; Sheng et al., 2024), or specific scattered phases such as P–S (e.g., Y. Lu and Ben-Zion, 2021), has helped improve the spatial

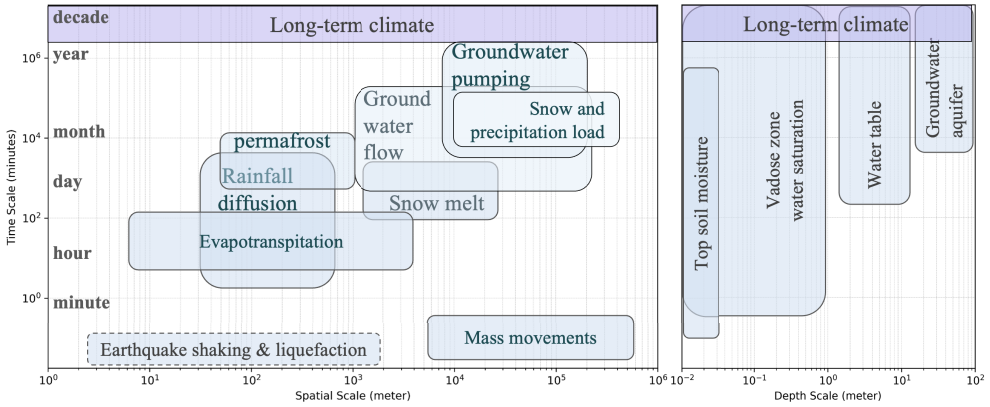

Figure 1. Range of spatial and time scales of the hydrological processes reported in the literature. Left: lateral spatial extent ranging from centimeters to 1000 km. Right: depth scale from centimeters to 100 m. Solid boxes represent the range of time and spatial scales where seismic signatures correlate with specific hydrological processes. Long-term climate effects have been reported at all spatial scales and depths.

localization of velocity changes. However, the use of ballistic waves for monitoring requires some knowledge about stability and location of repeated anthropogenic sources (e.g., trains, Higueret et al., 2024). In addition, coda waves are more sensitive than ballistic waves to small changes in $\mathrm{d}v/v$, as they sample the medium many more times due to multiple scattering (Snieder, 2002; Colombi et al., 2014). With the assumption that the scatterers themselves do not change positions, the perturbation of the seismic velocity averaged along the coda wave path is linearly proportional to the accumulated phase shift: $\mathrm{d}v/v = -\mathrm{d}t/t$, where t is the phase lag and $\mathrm{d}t$ is the phase shift in the coda (Poupinet et al., 1984). This review focuses on the observations made with coda waves but will highlight the potential for ballistic wave analysis in relevant cases. Beyond resource monitoring, many of the most damaging natural hazards, such as landslides, earthquake-induced liquefaction, and nonlinear site amplification, are also governed by hydromechanical processes in the Critical Zone. These hazards arise from the same physical mechanisms discussed throughout this review: changes in effective stress, pore pressure, saturation, and soil structure. In particular, the response of near-surface soils to strong shaking is modulated by water content and stress history, linking seismic hazard to hydrological variability. By framing these hazards as manifestations of CZ dynamics, ambient field seismology offers a unifying observational approach: the same seismic observables (e.g., $\mathrm{d}v/v$, attenuation (Q), and the Horizontal-to-Vertical Sprectral Ratio (HVSR)) used to track groundwater or vadose (unsaturated) processes can also be used to detect precursors to slope failures, assess site amplification conditions, and evaluate liquefaction susceptibility. This review aims to bridge these application areas and demonstrate how environmental seismology contributes to an integrated understanding of both hydrogeophysical processes and geohazards in the CZ.

1.2. *Seismic structure of the near surface*

The seismic structure of the shallow subsurface, especially in the critical zone, is marked by a surface low-velocity zone with shear wavespeeds (V_S) ranging from 130–1000 m/s spanning unsaturated and saturated soil, densities ranging from 1.7–2 g/cm^3, and P wavespeed (V_P) of 350–2500 m/s (e.g., Befus et al., 2011; Boore, 2016; Nagashima and Kawase, 2021). The shallowest layers are often highly weathered and have a greater sensitivity to hydrological processes at and above the water table depth than more consolidated sediments (Anderson et al., 2013; Okay and Özacar, 2023). Scattering attenuation in sediments, generated by higher porosity and crack density in shallow sediments, is often equal to or greater than intrinsic attenuation, which is dispersed as heat (Jemberie and Langston, 2005; Eulenfeld and Wegler, 2016; Y.-P. Lin and Jordan, 2023). Combined intrinsic anelastic and scattering effects may yield strong attenuation in shallow sediments, with total

quality factors (Q) as low as 2–10 for S and P waves in shallow soils (Malagnini, 1996).

2. Relating seismic properties to water content

Relating seismic measurements into hydrological processes requires understanding three topics: (1) **hydrological data** and, when lacking measurements, how seismologists infer it; (2) **rock physics models** to estimate elastic and anelastic properties with varying water content; (3) **seismic wave spatial and depth sensitivities** depending on the wave types.

2.1. *Hydrological models*

Water content, either in the form of water saturation or pore pressure, is a key element in the hydromechanical response of the critical zone. Due to the logistical challenges of obtaining high-resolution in situ measurements of water content and the resulting sparsity of data coverage, numerical and process-based models are often used to understand hydrological processes within the critical zone. The water budget includes sources (precipitation, snow melt, and runoff from uphill) and sinks (drainage, runoff, evapotranspiration).

The main approach that seismologists have used to estimate pore pressure in the fully saturated regime is through coupling infiltration from rainfall or snow melt with simplified outflow models based on either baseflow (Sens-Schönfelder and Wegler, 2006; Feng, Huang, Hsu, et al., 2021) or the poroelastic response to surface water input (E. Roeloffs, 1996; E. A. Roeloffs, 1998; Talwani et al., 2007; Tsai, 2011; Andajani et al., 2020; Q.-Y. Wang, Brenguier, et al., 2017). For regions with a significant soil moisture reservoir, the antecedent precipitation index has been used to represent the capacity of the vadose zone (Illien, Andermann, et al., 2021). Clements and Denolle (2023) found that baseflow and poroelastic-based models of pore pressure, along with the cumulative deviation from the moving mean of precipitation (Smail et al., 2019), equally worked as long-term proxies of groundwater level when compared to hydrologically-induced $\mathrm{d}v/v$.

Hydrological models that account for the full water budget with inputs and outputs (runoff, downward drainage, and evapotranspiration) are more conducive to modeling vadose zone dynamics. Lecocq et al. (2017) modeled water storage as a budget between input (precipitation) and output (river runoff and evapotranspiration) over a time period of three decades. Z. Shen et al. (2024) modeled water storage as a mass balance between precipitation (input), evapotranspiration modulated by surface moisture measurements and temperature (output), and deep water drainage (i.e. groundwater downward draining as an output). Additionally, groundwater levels can be inferred from river (Rodríguez Tribaldos and Ajo-Franklin, 2021) or lake (Clements and Denolle, 2023) levels, as surface body water levels are often hydraulically connected to the groundwater table.

2.2. *Hydromechanical models of Earth materials*

Theoretical, laboratory, and field studies have demonstrated that both V_P and V_S vary with water saturation in rocks (Nur and Simmons, 1969; O'Connell and Budiansky, 1974; Kuster and Toksöz, 1974). In partially saturated rocks, seismic velocity perturbations caused by changes in water content are controlled mainly by the density effect. Increasing bulk density through water saturation, achieved by replacing air with water, results in a gradual reduction in both V_P and V_S. When the rock achieves nearly fully saturated conditions (80%–90%), the non-compressibility of the fluid in the pores dominates the density effect, and V_P experiences a sharp increase. Commonly, V_S continues to decrease with saturation. In a few laboratory cases, however, studies have shown that a small increase in V_S can also be observed when saturation is close to 100%, which may be due to the effect of surface tension in small pores causing an increase in the shear rigidity of the rock (Knight and Nolen-Hoeksema, 1990). This increase in V_P and V_S at full saturation will mostly be observed near the water table and the capillary fringe. Beyond this general behavior, studies have shown that other hydrological processes can influence the behavior of seismic velocities in the unsaturated zone (e.g., see below discussion of Section 5.1). For example, strong matric suction effects can lower the effective stress and cause a consequent increase in V_P, which competes against the V_P reduction caused by the density effect (Linneman et al., 2021).

Below the water table, under **fully saturated** conditions, pore structure controls the relative change

in seismic velocity. For low-porosity rocks with crack-shaped pores, V_P increases with full saturation, whereas V_S remains unchanged with saturation (Nur and Simmons, 1969). For high porosity rocks with circular pores, V_P increases with saturation whereas V_S decreases with saturation (Toksöz et al., 1976). At shallow depths, where confining pressure is low, increases in pore pressure thus increase V_P and decrease V_S. At the near-surface, Rayleigh waves are far more sensitive to variations in V_S than V_P (Song et al., 1989). Thus, numerous observations have been made of a decrease in Rayleigh wave speed (V_S) with increasing groundwater levels or pore pressure. The constitutive relations for nonlinear elasticity show that relative change in elastic wavespeeds, $\mathrm{d}v/v$, is proportional to the dilatational strain ϵ_{kk} (Murnaghan, 1937; Ostrovsky and Johnson, 2001), and observations suggest that:

$$\mathrm{d}v/v = -\beta\epsilon_{kk}, \tag{1}$$

where β is in the range 1×10^3–1×10^4 (see compilation of values by Clements and Denolle (2023) and a more general formulation by Y. Wang et al. (2024)). Because pore pressure induces dilatational strains through poroelastic effects, hydrologists have found linear relationships between dilatational strains and hydraulic head ($S_{sk}\approx 1\times10^{-5}$, Burbey (2001)), $\epsilon_{kk} = S_{sk}\,\mathrm{d}h$, such as

$$\mathrm{d}v/v = -\beta s_{sk}\,\mathrm{d}h. \tag{2}$$

These relationships give a sensitivity of $\mathrm{d}v/v$ to water levels such that local wavespeed changes by 1–10% for 1 m of water change. Rivet et al. (2015) also proposes the alternative relationship that

$$\mathrm{d}v/v = \mathrm{cov}(\mathrm{d}v/v, p)/\mathrm{var}(p), \tag{3}$$

where p is the poroelastic pressure response to a point source of rainfall. This relation has been used in several studies comparing temporal changes in $\mathrm{d}v/v$ and near-surface (Delouche and Stehly, 2023; Barajas, Poli, et al., 2021).

In the **partially saturated** regime, above the water table, partial saturation effects on seismic wavespeeds are less trivial. The first-order effect is the change in density that occurs by replacing the air in the pores with water:

$$\rho = (1-\phi)\rho_s + \phi(S_w\rho_w + (1-S_w)\rho_a), \tag{4}$$

where ϕ is porosity, the densities of the host rock, water, and air are ρ_s, ρ_w, ρ_a, and saturation in the pores is S_w. Capillary forces also effectively increase the rigidity and bulk modulus of the material, such that effective V_P and V_S increase in the vadose zone (Solazzi et al., 2021). Additionally, Sakaki et al. (2010) demonstrated that water retention creates a dynamic sensitivity to capillary pressure, which is proportional to the rate of saturation change. This results in increased capillary pressure during drying cycles and decreased capillary pressure during wetting cycles. With increased saturation with depth, the competing factors of overburden pressure with static capillary forces yield a relatively constant V_P/V_S ratio down to the water table depth (Solazzi et al., 2021), below which V_S remains low in fully saturated media, V_P jumps to high values greater than the sound speed in the water, yielding a high V_P/V_S ratio, high Poisson's ratio and the sensitivity of Rayleigh wavespeed discussed above. Solazzi et al. (ibid.) found a particularly strong sensitivity of Rayleigh wavespeed to the partial saturation in medium-to fine-grained soils (see Figure 2), though larger pore sizes in concrete samples exhibited increased sensitivity of $\mathrm{d}v/v$ to saturation (Diewald et al., 2024). There is empirical evidence that such sensitivity remains relatively constant for the middle range of saturation (e.g., 30–80%). Still, dynamic capillary effects are much stronger at lower and higher saturation levels (Dong and N. Lu, 2016; Diewald et al., 2024; Sakaki et al., 2010).

It should be noted that V_S's sensitivity to water level greatly depends on the lithology: it is strong for clays but small for sand (Dong and N. Lu, 2016). Such a difference may explain why most seismological studies exhibit spatially variable sensitivity.

Changes in seismic attenuation, Q, in the partially saturated zone are less obvious. P-wave attenuation is greatly sensitive to partial saturation due to the contrast in the compressibility of mixed fluids (air vs. water) (e.g., Chapman et al., 2021; Amalokwu et al., 2014), whereas S waves are insensitive to compressible fluids. Numerous studies have correlated values of $Q_p/Q_s \leq 1$ with the presence of air/gas in a partially saturated medium (e.g., Hudson et al., 2023). Nevertheless, theoretical and empirical (Winkler and Nur, 1982; Diewald et al., 2024) studies have shown that S-wave or S-wave-dominated seismic attenuation varies with saturation. Seismic attenuation within partially saturated porous materials is mainly caused by the relative movement between the solid

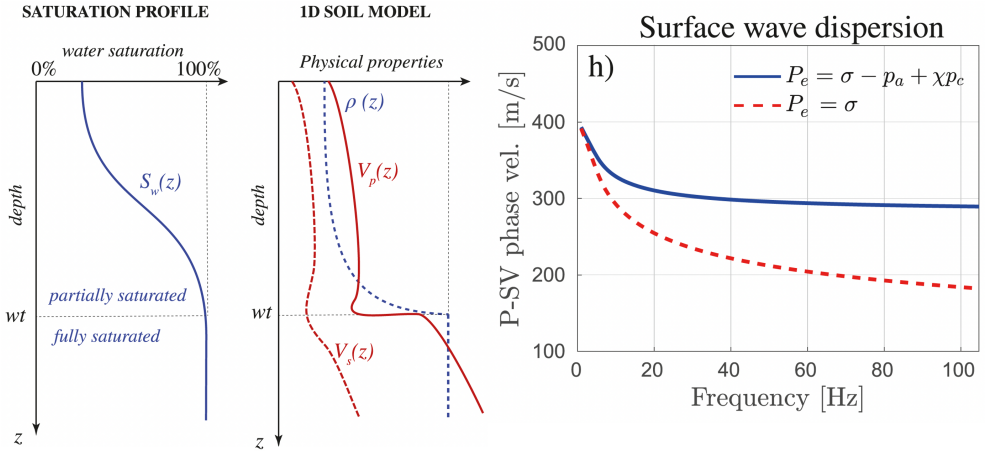

Figure 2. Generic seismic profile of a critical zone from Solazzi et al. (2021). Left plot: saturation increases from the surface until the water table (left). Middle plot: elastic physical properties (density ρ, P wave velocity V_P, S wave velocity V_S) as a function of depth. Right plot: Surface wave dispersion as a function of frequency with (blue lines) and without (red dashed lines) capillary forces included in the model. Solazzi et al. (2021) showed that when the V_P/V_S ratio, which is usually a metric for water content, is about constant in the partially saturated zone, surface wave velocities are sensitive to saturation due to capillary suction effects.

matrix and the pore fluid. This movement generates shear stresses in the fluid, leading to energy loss through viscous friction (Mavko and Nur, 1979).

2.3. *Wave types and their various spatial and depth scales*

Direct ballistic waves can be used to probe large changes in the subsurface, as phase shifts in the direct waves may be precise enough to estimate the seismic velocity changes. By using direct waves, the localization of the velocity perturbation is achieved simply through time-lapse tomography. Using ambient noise seismology, studies have focused on time-lapse shear wave tomography using surface wave dispersion curves (e.g., Dou et al., 2017; Mordret et al., 2020; Cheng et al., 2022; Sun et al., 2025). The typical frequencies used in these analyses range from 2 to 15 Hz, providing sensitivity to the shallow seismic structure from a few meters to approximately 40–50 m in depth. The spatial resolution of these measurements is typically on the order of tens of meters. Ballistic wave-based tomograpy is limited by the density of the seismic channels and the quality of the high-frequency signals. Besides surface waves, several studies have leveraged distinct seismic phases, such as refracted P waves (Brenguier, Courbis, et al., 2020) or converted phases (Y. Lu and Ben-Zion, 2021), when possible. One key element of using ballistic waves is that their spatial and depth sensitivity depends on the source-receiver geometry and the Earth's structure (ibid.). Because time-lapse tomography, which infers absolute seismic velocities in space (laterally and in depth) and time, rock physics models can extract temporal and spatial variations in hydro-thermo-mechanical properties of the critical zone (e.g., Sun et al., 2025).

When distinct seismic phases are undistinguishable or when the changes are subtle, seismologists use coda waves instead to image changes in the subsurface. Because scattered waves accumulate travel-time perturbations due to changes in seismic velocities, phase shifts are increased in late coda waves. For homogeneous velocity perturbations, such delays accumulate linearly regardless of the wave type involved (e.g., Obermann, Planès, Larose, et al., 2013).

The depth sensitivity of coda waves is most often assumed to be that of fundamental mode Rayleigh wavespeed, given a perturbation in V_S as a function of depth and frequency. Sensitivity kernels, which link observed wavespeed perturbations ($\mathrm{d}v/v$) to

true V_S perturbations between seismic stations often rely on solutions from the radiative transfer model for short lag-time measurements (Pacheco and Snieder, 2005; Planès et al., 2014). A good rule of thumb is that the penetration depth of the Rayleigh wave is around one horizontal wavelength (Barajas, Margerin, et al., 2022). When seismic velocity and density are relatively constant with depth, scattered body waves dominate the late coda of NCFs, though sensitivity kernels may couple surface and body wave sensitivity at depths below the critical zone (Obermann, Planès, Larose, et al., 2013; Obermann, Planès, Hadziioannou, et al., 2016; Obermann, Planès, Larose, et al., 2019; Margerin et al., 2019; Barajas, Margerin, et al., 2022).

3. Review of sensing technologies

We now focus on the technologies that have served the passive seismological community to investigate critical zone hydrology.

3.1. *Seismological observation networks*

3.1.1. *Permanent seismic networks*

The most commonly used sensors for ambient noise monitoring of the critical zone are broadband seismometers, typically deployed directly at the surface. Broadband seismometers have been deployed since the 1960s, although continuous digital recording began in the late 1990s. By 2002, most seismic networks had begun continuous recording of their entire broadband networks, which fueled the use of the ambient seismic field for seismological research (e.g., Campillo and Paul, 2003; Shapiro et al., 2005). The deployment of broadband sensors serves two purposes. First, the global detection and monitoring of explosions and earthquakes drive the deployment of these sophisticated stations worldwide, particularly on oceanic islands. With this purpose in mind, broadband sensors typically record at high gain to retrieve weak seismic waves from distant earthquakes and explosions. Second, regional and national seismic networks, with the specific goal of monitoring earthquake sources, have favored the deployment of broadband seismometers on bedrock and near fault zones. Because seismic waves amplify in soft sediments, network engineers have chosen to avoid these sites and focus on the station's sensitivity to fault zone waves. These locations are not ideal for subsurface hydrology, as the groundwater reservoirs and soils are predominantly located in basins. However, the advantages of broadband stations are their long-standing, multi-decadal, continuous records. Because their sensitivity spans a broad range of frequencies, seismologists have repurposed broadband seismometers to probe the near-surface in the 0.1–10 Hz frequency range, covering both powerful microseismic ambient fields and stationary anthropogenic seismic noise (e.g., Hasselmann, 1963; Díaz, 2016).

Accelerometers are also used for permanent seismic monitoring and typically record at lower digital gain to retrieve high fidelity of strong ground accelerations and higher frequencies (above 0.1 Hz). Regional seismic networks (e.g., the Southern California Seismic Network SCSN, the Northern California Earthquake Data Center NCEDC, and the Pacific Northwest Seismic Network PNSN) comprise several types of seismometers, ranging from broadband seismometers to accelerometers, for both monitoring microseismicity and early warning of strong earthquakes. Regional and global networks of seismometers (e.g., GSN, ORFEUS, Geoscope) archive their data on publicly accessible data servers, either on-premise servers or in cloud storage (e.g., E. Yu et al., 2021). Most of these installations are made at the surface only.

Several observatories *pair surface with borehole instrumentation* enabling top and bottom analysis of the near-surface environment. After the 1995 Hyogoken Nanbu Earthquake, NIED (National Research Institute for Earth Science and Disaster Prevention) constructed an uphole/downhole observation network, KiK-net (Kiban Kyoshin network), with approximately 700 stations (Aoi et al., 2004). Each KiK-net station has a borehole of 100 m or more at depth, and accelerometers have been installed both on the ground surface and at the bottom of the boreholes. Such pairs of sensors enable direct measurement of near-surface dynamics or physical properties between the two sensors. The KiK-net accelerometers in Japan have been unrivaled by other downhole networks in the volume of available acceleration seismograms, given the quality, homogeneity of the information describing subsurface layers, and the rate of seismicity. In addition to national observatories, another model for focused surface-to-borehole

observations exists in the geotechnical community, referred to as "liquefaction arrays". In the United States, such arrays include the Wildlife Liquefaction Array (Holzer and Youd, 2007) and the "Seattle Liquefaction Array" (Steidl and Hegarity, 2017), which feature piezoelectric pore pressure sensors, along with several shallow borehole seismometers, to continuously sample water pressure and earth vibration.

Near-surface structure information of the site on which these seismic observations are made is sometimes available. For instance, the velocity profiles and geological information, as well as the observed records, are widely accessible on the NIED website. C. Zhu, G. Weatherill, et al. (2021) created an open-source site database that contains site characterization parameters directly derived from available velocity profiles, including average wave velocities, bedrock depths, and velocity contrast. Additionally, the site database includes topographic and geological proxies inferred from regional models or maps. Geotechnical arrays also typically conduct surveys of the seismic and hydrological structure (e.g., Youd et al., 2004).

3.1.2. *Temporary seismic arrays*

Most seismic imaging of the near-surface entails a small aperture array of a few 100 m with seismic channel spacing of a few meters. When analyzing deeper and larger groundwater reservoirs, such as aquifers in sedimentary basins, the analysis aperture may range from 10 km to 100 km. Given these spatial considerations, seismologists use direct or refracted P waves (e.g., Flinchum, Holbrook, et al., 2022), direct surface waves (e.g., Sobolevskaia et al., 2024; Sun et al., 2025), and coda waves dominated by multi-scattered S and surface waves (e.g., Z. Shen et al., 2024) to explore the spatial and temporal variations in the CZ seismic properties.

For temporary seismic deployments, low-cost geophones, called "nodes" such as the FairField 3C or the SmartSolo nodes, have also been used for short-term experiments to image and monitor water table, precipitation, soil moisture, or seasonal frozen ground freeze–thaw cycles using seismic methods (Oakley et al., 2021; Hua et al., 2023; Gochenour et al., 2024; H. Liu et al., 2025; Behm et al., 2019; Hua et al., 2023; Grobbe et al., 2021). Nodes are easy to deploy in "large-N" arrays, fast to install in rapid response to earthquakes or sudden environmental events; their disadvantage is a short battery life of a month that limits long-term monitoring.

A novel technology transforming the field of seismology, particularly in near-surface seismic imaging and monitoring, is distributed acoustic sensing (DAS). DAS technology transforms traditional fiber-optic cables into dense arrays of sensors, enabling the measurement of distributed strain or strain-rate changes along their length (e.g., Hartog, 2017). Current DAS technology can continuously record the seismic wavefield at a spatial resolution of a few meters along cable lengths that can exceed 100 km. Several studies have also demonstrated that DAS can record strain-rate signals over a broad range of frequencies, ranging from 0.01 to hundreds of Hertz (N. J. Lindsey et al., 2019; Paitz et al., 2020), though near-source, high ground motion observations are often "clipped" due to DAS's limited sensitivity at high strain rates (C.-R. Lin et al., 2025). The primary advantage of DAS lies in its capacity for continuous, real-time monitoring across extensive areas or structures sampling the wavefield over many closely spaced (~3–10 m) virtual channels using either pre-existing telecommunication fiber-optic cables or short-term fiber deployments. DAS measures strain rate along the axial direction of the cable, making it especially suitable for ambient noise studies, in which Rayleigh waves traveling along the axis of the cable can be analyzed for subsurface imaging and monitoring. DAS arrays produce substantial amounts of raw strain data ($\sim TB$s), which makes storing, sharing, and analyzing the data computationally difficult.

3.2. *Hydrological observations networks*

Seismologists have attempted to explain the hydrological signature by observing time-dependent seismic wavespeeds. Occasionally, in-situ measurements are possible near or at seismic stations, such as groundwater wells (e.g., C.-Y. Lin et al., 2024) or soil moisture probes (e.g., Illien, Andermann, et al., 2021; Oakley et al., 2021; Sobolevskaia et al., 2024). Typically, the distance between the seismometer and the in-situ hydrological sensor is up to a few kilometers, and the hydraulic conductivity between the two sites is either unknown or highly uncertain. Piezoelectric probes are frequently used to infer water levels and

have been employed in several local studies (Voisin, Guzmán, et al., 2017; Gaubert-Bastide et al., 2022).

Networks of groundwater wells are increasingly made available to the public (Goodall et al., 2008), such as the National Ground Water Monitoring Networks maintained in individual countries; however, data rights still pose challenges for data sharing (Condon et al., 2021). Overall, groundwater wells are either pumped for agricultural, domestic, or industrial uses or used to monitor groundwater levels (Margat and Van der Gun, 2013) passively. In the past, one challenge seismologists have faced in accessing groundwater well data to compare with their seismic proxies has been the decentralization of groundwater well observation networks and the non-uniformity in the temporal sampling of the wells.

Determining the soil moisture (SM) content of the CZ is crucial for effective resource management and hazard mitigation during extreme droughts and floods. There are several methods for inferring or measuring soil moisture. Babaeian et al. (2019) provides an extensive review of these approaches, which are categorized as remotely sensed (using satellite or airborne sensors), proximally sensed (e.g., GPS reflectometry), or terrestrially sensed (e.g., time-domain reflectrometry). These methods are only sensitive to the upper 50 cm, limiting analysis to the upper part of the critical zone and lacking sensitivity for deeper processes such as the weathered bedrock (2–30 m). Additionally, ground-based sensors are particularly local, while remotely sensed SM measurements typically have a footprint of 10s of kilometers: empirical downscaling strategies are often required to bridge the scales.

When lacking in situ or remotely sensed measurements, seismologists have turned to inferring water content from a hydrological model (see Section 2.1). For example, Lecocq et al. (2017) used precipitation data together with a runoff, discharge, and evapotranspiration model to estimate groundwater storage.

4. Review of methodologies in seismology

4.1. *Active near-surface imaging with body waves*

Near-surface geophysics (NSG) typically refers to temporary experiments that involve deploying sensors, transmitting a source, and inverting data to determine water content and structural properties. NSG is a mature field of geophysics, with a vast set of methodologies and dedicated curriculum (Butler, 2005; Everett, 2013). Non-invasive methods for characterizing critical zone water content include electrical and electromagnetic surveys (Siemon et al., 2009), magnetic susceptibility and resonance methods (Hertrich, 2008), ground penetrating radar (Klotzsche et al., 2018), gravity survey (Gehman et al., 2009; Syed et al., 2008), and seismic, on which this review will expand.

Seismic methods for inferring near-surface water content typically use active seismic surveys and short-period seismometers (geophones) (Befus et al., 2011; Flinchum, Holbrook, et al., 2022). Usually, travel time measurements of the direct and refracted P waves are used to generate reflection and refraction images of the near-surface (Befus et al., 2011). The spatial scales of these surveys vary from 10 to 100s of meters, depending on the spacing of the geophones (e.g., Uecker et al., 2023; Flinchum, Grana, et al., 2024). Sophisticated methods, such as full-waveform inversion, which were initially developed to image regional-scale subsurface stratigraphy, are now being applied to the critical zone (X. Liu et al., 2022).

4.2. *Time-lapse surface wave tomography*

Surface waves are dispersive, and their dispersion relation depends on the vertical shear wave profile. Using either active or passive (e.g., ambient noise cross correlations) sources, surface wave imaging in near-surface geophysics has significantly advanced the monitoring of water content changes in the critical zone. By analyzing surface wave dispersion, these methods utilize the frequency-dependent velocity of Rayleigh waves to infer subsurface elastic properties, which are sensitive to variations in water content. Dispersion inversion techniques, such as multichannel analysis of surface waves (MASW) or the frequency-wavenumber method (Park et al., 1999), allow the creation of shear wave velocity profiles, and when repeated over time, they correlate with changes in soil moisture and porosity (Socco et al., 2010; Cheng et al., 2022; Sobolevskaia et al., 2024; Sun et al., 2025) or shallow aquifer structure (Gochenour et al., 2024; Eppinger et al., 2024).

4.3. *Changes in seismic velocity* $\mathrm{d}v/v$

The relative change in seismic velocity, $\mathrm{d}v/v$, derived from ambient noise cross-correlation is sensitive to near-surface changes in saturation, pore pressure, and overall effective stress. $\mathrm{d}v/v$ monitoring of hydrological changes in the critical zone spans from point measurements using single station cross-channel correlations (Sens-Schönfelder and Wegler, 2006; Donaldson et al., 2019; Kim and Lekic, 2019; Lindner et al., 2021; Feng, Huang, Hsu, et al., 2021; Clements and Denolle, 2023) to kilometer-scale variations using inter-station cross-correlations (Lecocq et al., 2017; Q.-Y. Wang, Brenguier, et al., 2017; Clements and Denolle, 2018; Mao, Lecointre, et al., 2022; Mao, Ellsworth, et al., 2025). We illustrate the clear evidence that $\mathrm{d}v/v$ correlates with water content in Figure 3.

The temporal resolution of the $\mathrm{d}v/v$ transient depends on the time scale of the process under study, which spans from seconds for earthquake shaking (Illien, Turowski, et al., 2025) and liquefaction (Viens, Bonilla, et al., 2022) to decades for climatic processes (Lecocq et al., 2017; Clements and Denolle, 2018; Mao, Lecointre, et al., 2022; Mao, Ellsworth, et al., 2025), as shown in Figure 1. For long-term monitoring studies and at regional scales, NCFs are averaged in 1–30 day moving windows to increase signal-to-noise ratio (SNR) (Seats et al., 2012), while other studies with short aperture may report sub-hourly temporal resolution in $\mathrm{d}v/v$ (Xie et al., 2023; Rodríguez Tribaldos and Ajo-Franklin, 2021). The non-stationarity of the seismic sources and their coherence is the main limiter of temporal resolution and robustness of $\mathrm{d}v/v$ measurements. Typically, short aperture arrays or single-station measurements can yield high temporal resolution (e.g., minutes to hours) at high frequency signals (e.g., Xie et al., 2023) while greater array aperture and lower frequency signals tend to become stable over longer time periods (e.g., days to months) (e.g., Mao, Ellsworth, et al., 2025; Clements and Denolle, 2023). Improving the quality and temporal resolution of cross-correlation is an area of research (A. M. Baig et al., 2009; Hadziioannou, Larose, A. Baig, et al., 2011; Viens and Van Houtte, 2019; Yang et al., 2023; He et al., 2024). Retrieving dynamics at time scales shorter than minutes, ambient field seismology relies on the stationarity of the ambient field. It tends to be limited to single-channel analysis or near-sensor processes.

Coda waves multiply scatter in the subsurface and thus have increased, though still weak, sensitivity to perturbations in the medium (Colombi et al., 2014). Given that the sensitivity is weak, observed $\mathrm{d}v/v$ values typically under-predict the perturbation at depth (Obermann, Planès, Larose, et al., 2013; Obermann, Planès, Hadziioannou, et al., 2016; Barajas, Margerin, et al., 2022; Yuan et al., 2021). Furthermore, $\mathrm{d}v/v$ is measured as decreasing with lag time in the coda (e.g., Gassenmeier et al., 2014; Takano, Brenguier, et al., 2019), which is also expected from the low sensitivity of body waves to perturbations (Obermann, Planès, Larose, et al., 2013; Barajas, Margerin, et al., 2022).

$\mathrm{d}v/v$ can be measured in both the frequency and time domains. The moving window cross-spectral (MWCS) technique developed by Poupinet et al. (1984) and the stretching technique developed by Lobkis and Weaver (2003) and first used in an environmental context by Sens-Schönfelder and Wegler (2006) are the most commonly used methods in the frequency and time domains, respectively. The stretching technique works well at low SNR levels (Hadziioannou, Larose, Coutant, et al., 2009), whereas the MWCS is computationally faster to calculate (Clarke et al., 2011). Recently Okubo et al. (2024) found that the stretching and MWCS methods may yield different results depending on which scattered wave dominates in the coda. Additionally, Mikesell et al. (2015) developed a method based on dynamic time warping to measure local phase shift measurements in the coda, Mao, Mordret, et al. (2019) developed a wavelet-based method to measure phase shifts, and Yuan et al. (2021) suggested combining the wavelet and stretching techniques to improve the frequency-dependence of the measurements relative to all previously stated methods. Overall, studies have attempted to measure $\mathrm{d}v/v$ over a range of seismic frequencies, which is desirable in the attempt to estimate the depth of the changes.

4.4. *Changes in seismic attenuation*

Attenuation is highly sensitive to water content, but is always comprised of two effects, intrinsic attenuation and scattering attenuation, which are

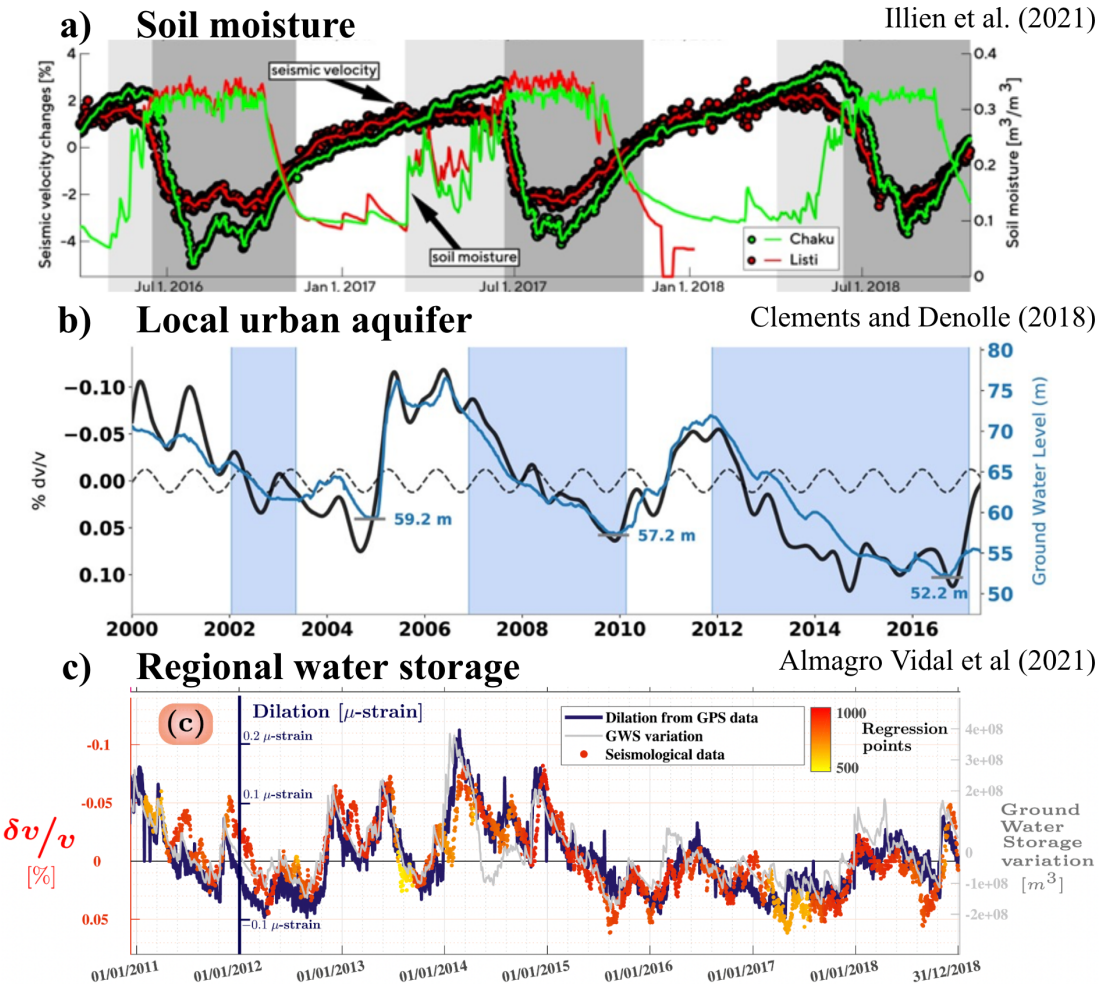

Figure 3. Temporal evolution of $\mathrm{d}v/v$ relative to water storage seen for (a) soil moisture (green and red lines) by Illien, Andermann, et al. (2021), (b) groundwater (blue line) by many, including Clements and Denolle (2018), and (c) in regional-scale karstic groundwater storage (gray line) by Almagro Vidal et al. (2021).

often difficult to disentangle in observations. A first method for measuring attenuation as related to fluids estimates the amplitude decay as a function of distance in the frequency domain through direct single wave measurements (e.g., Hudson et al., 2023) or using the exponential decay in the spectral autocorrelation method (e.g., Aki, 1957; Prieto et al., 2009; Nakahara, 2012; Lawrence et al., 2013). Another class of methods proposed by Malagnini et al. (2022) utilizes a generalized inverse technique for regression among pairs of earthquakes and stations. A second method for attenuation measurements focuses on the waveform envelope shape for which the radiative transfer theory (Sato et al., 2012; Mayor et al., 2014) is frequently used to model the dissipation of seismic energy and incorporate explicit functional forms for intrinsic and scattering attenuation, which may be necessary to extract the seismic signature of fluids (e.g., Hirose, Nakahara, et al., 2019; Hirose, Ueda, et al., 2022; Hirose, Q.-Y. Wang, et al., 2023; van Laaten and Wegler, 2024). Overall, measurements are made with absolute values of attenuation and evaluated over time. Recently, Pinzon-Rincon et al. (2025) observed 5% variations of seismic attenuation due to changes

in shallow water storage in the first tens of meters of the subsurface (12–23 Hz).

4.5. *Changes in ground motion site response*

The response of the near-surface to incoming earthquake ground motions is referred to as "site response" or "site effects", and they often include linear effects of wave propagation in the shallow soil layers and the damage and nonlinear deformation of these materials when ground motion amplitudes are sufficiently high. Site effects arise due to the presence of impedance (the product of wave velocity and density) contrasts and subsurface topographies. Site effects also depend on the attenuation of waves in the near-surface environments. Modeling site effects, therefore, requires in-depth knowledge of the site's velocity structure and the various factors controlling attenuation.

Site response can be precisely measured using instrument-based methods, such as spectral ratio (SR) techniques (Borcherdt, 1970), the generalized inversion technique (GIT, Andrews, 1986), and residual analysis (Abrahamson and Youngs, 1992), within ground motion models (GMMs). SR methods require a reference-target recording pair, such as a borehole station or a station on subsurface reference rock. In contrast, GIT and GMM residual analysis depend on a regional seismic network that includes the site of interest and has recorded multiple past earthquakes with comprehensive azimuthal and distance coverage. SR methods have also been utilized for measuring the environmental impacts on slope stability (e.g., Borgeat et al., 2024).

Where direct measurement or modeling is not possible, amplification can be predicted by generic prediction models linking amplifications to various predictor variables. Predictive variables can be site parameters from in situ geotechnical/geophysical measurements, e.g., shear wave velocity in the shallowest 30 m (V_S30), sediment thickness, and site resonant frequency (e.g., Hassani and Atkinson, 2017; Kwak and Seyhan, 2020) or indirect data from existing regional models or maps, such as topographic slope, terrain and geology (e.g., Wald and Allen, 2007; G. A. Weatherill et al., 2020). These indirect methods have recently shown good performance at predicting site response due to the emergence of quality databases and the associated use of machine learning methods (C. Zhu, G. Weatherill, et al., 2021; C. Zhu, Cotton, Kawase and Nakano, 2023; C. Zhu, Cotton, Kawase and Bradley, 2023).

Another metric of site response is the horizontal-to-vertical spectral ratio (HVSR). HVSR identifies fundamental resonance frequencies of soil layers, aiding in seismic microzonation, site amplification studies, and subsurface characterization (Nakamura, 1989). It is particularly valuable for evaluating the thickness and stiffness of sediments, seismic hazard assessment, and earthquake-resistant design (see review by Molnar et al., 2018). The influence of environmental variations on site responses is just beginning to be explored (e.g., Vassallo et al., 2022; Kula et al., 2018; Colombero et al., 2018). Händel et al. (2025) have also identified seasonal variations of high-frequency ground motion characteristics in northeastern Hokkaido and Honshu.

5. Seismic monitoring of hydrological resources and hazards

5.1. *Vadose-zone dynamics*

Seismological methods offer valuable insights into the partially saturated vadose zone, where complex water dynamics, including infiltration, evapotranspiration, drainage, and runoff, interact with the mechanical properties of near-surface soils and rocks. These processes have been modeled using a range of hydrological and poroelastic frameworks, and increasingly constrained by seismic observations of velocity changes ($\mathrm{d}v/v$) that respond to water saturation and stress conditions.

Several studies have used seismological data to **model hydrological processes**. For instance, Fores et al. (2018) modeled $\pm 0.2\%$ $\mathrm{d}v/v$ variations in the 6–8 Hz frequency band by integrating a water budget, including rainfall, evapotranspiration, and drainage, with gravity data and Biot-Gassmann-based petrophysical models, effectively tracking changes in water saturation in a karstic setting. Similarly, Illien, Andermann, et al. (2021) developed a two-layer hydrological model incorporating an antecedent precipitation index and rainfall thresholds to explain $\pm 2\%$ $\mathrm{d}v/v$ variations in the 4–8 Hz frequency range driven by transpiration and runoff. Their model effectively captured responses to heavy monsoonal precipitation in Nepal. In permafrost settings,

Sobolevskaia et al. (2024) and Sun et al. (2025) analyzed $\mathrm{d}v/v$ in terms of thermoelastic, poroelastic, and saturation-driven processes caused by thawing, precipitation, and air temperature variations.

Vadose zone seismology has been enabled by both **long-term sparse networks** and **short-term dense deployments**. The Crépieux–Charmy water exploitation site in France exemplifies a long-term test bed where ambient noise seismology has been combined with hydrological observations using permanent and temporary densified arrays, as well as piezo-electric sensors (Voisin, Guzmán, et al., 2017; Garambois et al., 2019; Gaubert-Bastide et al., 2022). The Susquehanna Shale Hills Critical Zone Observatory in the United States has supported year-round seismic monitoring to detect shallow responses to meteorological and hydrological forcing (Oakley et al., 2021). More recently, dense distributed acoustic sensing (DAS) deployments have enabled higher spatial resolution. For example, several studies used DAS to detect sub-seasonal $\mathrm{d}v/v$ decreases following precipitation and long-term increases associated with drying, with a depth sensitivity down to 150 m in semi-arid eastern California and in permafrost regions of Alaska (Z. Shen et al., 2024; Sobolevskaia et al., 2024; Sun et al., 2025).

Interpreting vadose zone dynamics requires careful attention to the differential sensitivity of seismic waves to fluid and matrix properties. S waves are particularly responsive to changes in effective stress and soil stiffness. Garambois et al. (2019) found an approximately linear relationship of a 1% drop in S-wave $\mathrm{d}v/v$ and 1 m increase in water table height at frequencies above 5 Hz, although with deviations from that linear relation with a hysteresis observed during wetting and drying (e.g., Garambois et al., 2019; Gaubert-Bastide et al., 2022; J. Shen and T. Zhu, 2025) can be explained with capillary effects in the partially saturated zone (Dong and N. Lu, 2016; Solazzi et al., 2021). In contrast, P-wave velocities are more sensitive to changes in fluid compressibility; in the same study, increases in P-wave velocity were attributed to greater saturation and reduced pore compressibility. Shallow monitoring studies, such as Oakley et al. (2021) and Sun et al. (2025), further highlighted that near-surface P-wave velocities may also respond to thermoelastic effects caused by temperature fluctuations and moisture changes in the top few meters. DAS technologies, which primarily sense strain rates related to mixed wave modes, offer a promising avenue to observe these joint sensitivities over depth and time (Z. Shen et al., 2024; Sobolevskaia et al., 2024; Sun et al., 2025).

5.2. *Groundwater resource management*

Groundwater monitoring with $\mathrm{d}v/v$ is a developing technique for water resource management at the aquifer scale. There is a strong anti-correlation between $\mathrm{d}v/v$ and relative changes in groundwater levels, i.e., when groundwater levels decrease, $\mathrm{d}v/v$ increases and vice-versa. Clements and Denolle (2018) showed that an increase of up to 16 m of groundwater level over a $\sim 20 \times 40$ km area during the winter of 2004/2005 was commensurate with a 0.15% decrease in $\mathrm{d}v/v$ in the 0.5–2.0 Hz frequency range (sensitivity to ~500 m depth). Spatial changes in $\mathrm{d}v/v$ and groundwater level were the largest in the deepest part of the basin. Mao, Lecointre, et al. (2022) compared $\mathrm{d}v/v$ and groundwater levels over the $\sim 40 \times 80$ km greater Los Angeles coastal aquifers in the 0.5–2.0 Hz frequency band (sensitivity to ~350 m depth). They measured a long-term increase of up to 0.2% $\mathrm{d}v/v$ in the central Los Angeles (LA) basin associated with groundwater pumping from 2000–2020. Whereas the Santa Ana basin with active groundwater replenishment had a 0.2% decrease in $\mathrm{d}v/v$. Almagro Vidal et al. (2021) measured $\mathrm{d}v/v$ in the 0.7–0.9 Hz frequency range (depth sensitivity to ~200 m) over an area of $\sim 60 \times 60$ km in Northern Italy. They found that 0.05% $\mathrm{d}v/v$ variations were correlated to 1×10^8 m^3 changes in total groundwater storage in a karstic aquifer. At a much smaller spatial scale ($\sim 500 \times 500$ m area) in the Crépieux–Charmy field site, Gaubert-Bastide et al. (2022) measured a 3% decrease in $\mathrm{d}v/v$ in the 2–5 Hz frequency range corresponding to a 3 m increase in groundwater level. Figure 4 shows the progress of increasing the spatial resolution of groundwater monitoring with $\mathrm{d}v/v$ for water management.

Beyond measuring relative changes in groundwater levels, seismological studies have attempted to infer groundwater dynamics. For example, Delouche and Stehly (2023) found that deep karstic and confined aquifers had a rapid response to seasonal rain (30–60 days) and a reduction in velocities. Mao, Ellsworth, et al. (2025) found that intense rainfall events during the 2023 winter storms

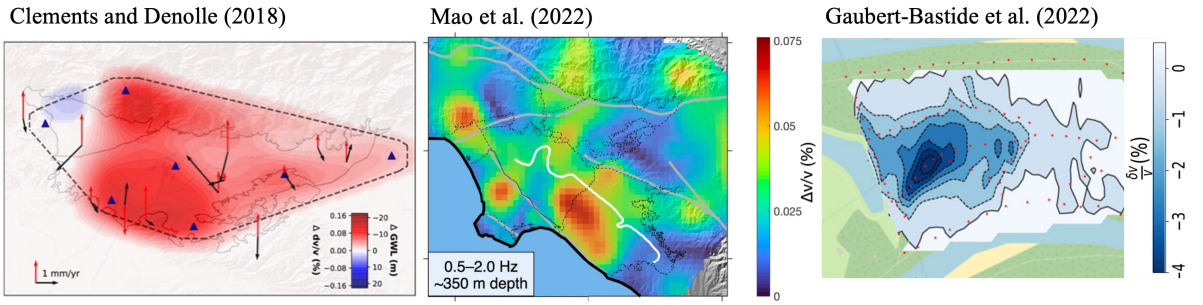

Figure 4. Using seismological proxies to groundwater levels. Left: Clements and Denolle (2018) first developed a smooth map of groundwater level change in the San Gabriel basin, CA. Spatial extent: ~20 × 60 km. Middle: Mao, Lecointre, et al. (2022) mapped $\mathrm{d}v/v$ at 2 × 2 km with 2D sensitivity kernels in the greater Los Angeles, CA area. Spatial extent: ~40 × 80 km. Right: Gaubert-Bastide et al. (2022) mapped $\mathrm{d}v/v$ at 20 × 20 m in the Crépieux–Charmy field site, Lyon, France. Spatial extent: ~500 × 500 m.

in California replenished shallow aquifers but not the deep aquifers that are the main contributors to Calfornia's water storage.

5.3. *Landslide monitoring*

Landslide dynamics are profoundly affected by subsurface hydrology (Greco et al., 2023). Rapid changes in the stress field or the water storage, e.g., due to massive rainfall events or earthquake shaking, are often causes for slope failures (Dai et al., 2002). Because hydrological data alone do not always correlate with landslide movements (Schulz et al., 2018), additional information about the rheology and transient processes, such as heterogeneous soil swelling in shear zones (ibid.) or rheological and hydrological heterogeneity (Tacher et al., 2005), is required. The pioneering work of Mainsant et al. (2012) demonstrated that pore-pressure-driven $\mathrm{d}v/v$ decreased 7% in the 10–12 Hz frequency range in the four days preceding a catastrophic landslide. Since then, ambient noise monitoring has become a popular way to monitor continuously and forecast landslides: Le Breton et al. (2021) recently provided a comprehensive review of how ambient noise monitoring has been applied to and benefited landslide research, and in particular, the advantages and challenges in making the $\mathrm{d}v/v$ measurements robust at short time scales for monitoring landslides. More recently, researchers have monitored the water content in landslides, tailing dams, and unstable rock slopes with $\mathrm{d}v/v$, especially in response to rainfall events (Z. Liu et al., 2024; Ouellet et al., 2022; Borgeat et al., 2025). Marc et al. (2021) showed that the landslide susceptibility rate in the epicentral zones of large earthquakes followed a similar recovery as $\mathrm{d}v/v$ in the year following strong ground motion. Collins et al. (2024) used HVSR to estimate the thickness of the slow-moving Barry Arm landslide. Overall, ambient noise methods provide in-situ, high temporal resolution monitoring of the coupled mechanical and hydrological processes that drive landslides. These ground failures, whether triggered by seismic or hydrological loading, should be viewed as dynamic responses of the critical zone, where stress redistribution and fluid–solid coupling govern stability.

5.4. *Seismic hazards*

Site effects can significantly impact seismic hazards by amplifying seismic waves and altering soil behavior in the shallow subsurface (i.e., the upper ~50 m). Under weak ground motions, shallow soil layers typically behave in a linear elastic manner, with amplification primarily dependent on the incoming seismic wave strength. During strong shaking, soft soils may undergo substantial dynamic strains and exhibit non-linear responses (Ishihara, 1996). This nonlinearity often results in a relative de-amplification of high-frequency ground motions and a shift of energy toward lower frequencies (Beresnev and Wen, 1996). Numerous studies have highlighted the potential of seismic interferometry to monitor the nonlinear behavior of shallow sediments from single

seismometers (Bonilla and Ben-Zion, 2020; Hobiger et al., 2014; Hobiger et al., 2016; Viens, Denolle, et al., 2018; Esfahani et al., 2024), surface-borehole arrays (Bonilla, Guéguen, et al., 2019; Nakata and Snieder, 2011; Qin et al., 2020), and DAS arrays (Viens, Bonilla, et al., 2022). $\mathrm{d}v/v$ can decrease as much as 50–60% in the few seconds following strong motion at frequencies above 1 Hz (Bonilla, Guéguen, et al., 2019). In extreme cases, phenomena such as liquefaction (Nakata and Snieder, 2011), dynamic compaction (Viens and Delbridge, 2024), and significant variations in soil stiffness and strength (Chandra et al., 2015) have been observed. Recent studies have also highlighted the impact of environmental changes, such as rainfall and freeze-thaw cycles, on the subsurface response to ground motions (Roumelioti et al., 2020; Händel et al., 2025). Importantly, seismic hazard itself, via liquefaction and ground failure, is a hydromechanical outcome of CZ processes, reinforcing the need for an integrated perspective.

5.5. *Permafrost*

Permafrost, which underlies vast areas of the Northern Hemisphere and other cold regions, is warming at an increasing rate due to climate change. The degradation of permafrost poses significant risks, including the release of greenhouse gases such as methane and carbon dioxide, which further exacerbate global warming, as well as threats to ecosystems, hydrology, and infrastructure (Biskaborn et al., 2019). Conventional monitoring systems include temperature measurements through the Global Terrestrial Network for Permafrost and conventional active geophysics surveys, such as resistivity and ground-penetrating radar (Kneisel et al., 2008). Environmental seismology has demonstrated great potential in monitoring permafrost phenomena, mainly through the $\mathrm{d}v/v$ and HVSR methods. $\mathrm{d}v/v$ monitoring constrains the timing of seasonal freeze and thaw in the active layer, which comprises the upper layer of soil. Thawing of the active layer in early summer induces a 5–10% drop in $\mathrm{d}v/v$ at frequencies of 1–30 Hz, whereas refreezing in the late fall increases $\mathrm{d}v/v$ a similar amount (James, Knox, Abbott and Screaton, 2017; James, Knox, Abbott, Panning, et al., 2019; Guillemot, Helmstetter, et al., 2020; R. Steinmann, Hadziioannou, et al., 2021; James, Minsley, et al., 2021). This 5–10% $\mathrm{d}v/v$ drop is much less than ~75% difference in velocity between the unfrozen active layer and the frozen permafrost body (Kneisel et al., 2008), which suggests that most $\mathrm{d}v/v$ studies are sensitive to depths deeper than the active layer. Seasonal fluctuations in the thickness of the active layer also lead to a sharp velocity contrast at the active layer-permafrost boundary, which can be monitored with the HVSR on land (Kula et al., 2018; Weber et al., 2018; Köhler and Weidle, 2019) and in submarine environments (Overduin et al., 2015; Angelopoulos et al., 2024). In addition to seasonal variations in $\mathrm{d}v/v$, Albaric et al. (2021) and Lindner et al. (2021) recovered long-term decreases in $\mathrm{d}v/v$ in permafrost over 3 and 15 years, respectively, suggesting an expansion and warming of the active layer. DAS arrays deployed in permafrost allow for detailed inversion of permafrost structure using tomographic methods (Ajo-Franklin et al., 2017) and $\mathrm{d}v/v$ monitoring of both the timing and spatial extent of the freeze and thaw cycle (Cheng et al., 2022; Sobolevskaia et al., 2024). Recently, R. Steinmann, Seydoux, et al. (2022) employed an artificial intelligence-based method to identify the pattern of ground freezing from continuous ambient seismic noise in an urban environment, and Sun et al. (2025) utilized a rock-physics model to disentangle the relative contributions of thawing, precipitation, thermoelastic, and poreelastic stresses, each of which may dominate at specific depth ranges and depending on the water table depth (C. Yu et al., 2025).

5.6. *Snow load and melt*

The effects of snow load and melt on $\mathrm{d}v/v$ can be multi-faceted. Guillemot, van Herwijnen, et al. (2021) measured a 2–3% decrease in $\mathrm{d}v/v$ between 10–25 Hz after dry snowfall. They interpreted snowfall as adding new mass onto the surface without increasing the rigidity, thereby decreasing seismic velocity. In contrast, vertical loads induced by the weight of snow (and or pre-snow precipitation) have been interpreted with a positive increase in $\mathrm{d}v/v$ at frequencies below 10 Hz (Cannata et al., 2017; Makus et al., 2023). Heavy, wet snow has been interpreted as (1) increasing water content in the pores as correlated with snow-water equivalent thickness (Hotovec-Ellis et al., 2014) or (2) increasing pore pressure in fluid-filled cracks (Silver et al., 2007; Taira and Brenguier, 2016).

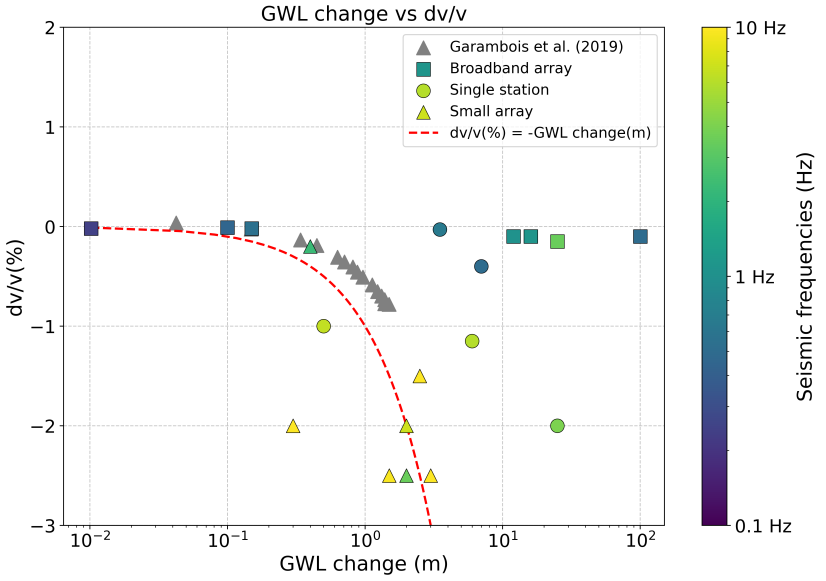

Figure 5. Change in seismic velocities as a function of groundwater level change. Values are shown from individual studies that reported water levels, or pore pressure, which we converted to water level change using a hydrostatic pressure $p = \rho g\, \mathrm{d}H$, where $\rho = 1000$ kg/m^3 and $g = 9.81$ m/s^2 the gravity constant. Squares represent values obtained from inter-station correlations from regional seismic networks with station spacing on the order of 10 km. Triangles are measurements made with inter-station correlations of small arrays of apertures of about 1 km. Circle markers are measurements obtained from single-station methods. Gray triangle is a digitally extracted data from Garambois et al. (2019). The color bar represents the middle of the frequency band used in each study. The dashed red line is simply showing $\mathrm{d}v/v = -$GWL without any fitting.

6. Summary of seismological evidence for ground-water hydrology

Our review highlights the ubiquitous correlation between groundwater levels, $\mathrm{d}v/v$, and other seismic markers. To achieve such a correlation, studies may have had to disentangle the hydrological signature in $\mathrm{d}v/v$ from other contributing factors (e.g., tectonic, thermoelastic) using modeled and/or observed data. From the numerous studies mentioned in this review, we collected the values of $\mathrm{d}v/v$, their corresponding $\mathrm{d}H$ groundwater level changes, the type of seismic network configuration, and the frequencies (i.e., depth) involved. Figure 5 shows how $\mathrm{d}v/v$ has been reported to vary against groundwater levels. The studies are compiled based on comparisons with aquifer or water-table levels. We categorize them based on the experimental setting: inter-station cross-correlations in regional seismic networks, small aperture arrays, or single-station measurements.

Overall, the simple relation $\mathrm{d}v/v(\%) = -\mathrm{GWL}(m)$ is strikingly accurate. The deviation from this relation is explained by the following: (1) a choice of inter-station correlations with large separation, and (2) the choice of a low-frequency band of analysis. Both settings yield a lower sensitivity of $\mathrm{d}v/v$ to perturbations at depth. The remaining variability is likely due to differences in lithology, as studies range from karstic carbonate environments to alluvial fans and large sedimentary basins. The sensitivity of shear waves to sediments is drastically different, especially between sand and clay (Dong and N. Lu, 2016).

7. Future directions and research priorities

7.1. *Bridging data gaps with enhanced sensor deployment*

Seismology is well-positioned to fill a hydrological data gap between remotely sensed observations and ground-based hydrological sensors, which have a

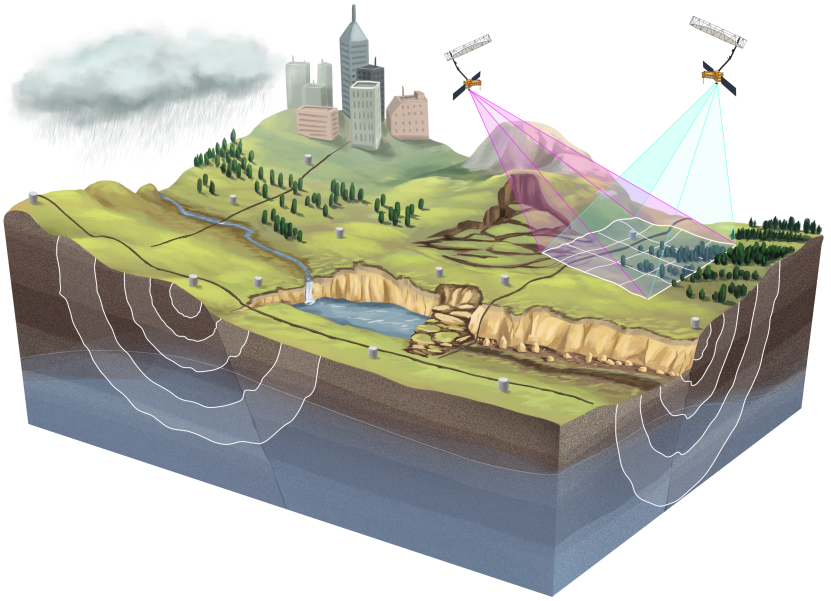

Figure 6. Critical Zone processes are probed by geophysical measurements through ground base sensors sensitive to the subsurface (seismometers, distributed acoustic sensing) and airborne or satellite measurements that probe the surface or very near surface properties. Art made by Elena Hartley.

spatial sensitivity of 10–100 m and a depth sensitivity of 1 cm to 100 m. Despite the recent progress in Earth observation, data gaps persist in the spatial distribution of seismic sensors at regional scales. Future studies should prioritize the co-located deployment of seismic and hydrological sensors to improve ground truth data and validate models. Multi-sensor data fusion will likely be a desirable mode of analysis (see Figure 6), such as supplementing critical zone observatories (e.g., CZO and OZCAR Brantley et al., 2017; Gaillardet et al., 2018) with added geophysical monitoring capabilities (e.g., seismic and geodetic networks). This approach will enhance our understanding of subsurface processes by directly correlating seismic observations with hydrological measurements. Emerging technologies, such as distributed acoustic sensing (DAS), could play a pivotal role in addressing this gap, enabling cost-effective, high-density sensor networks.

Additionally, it should be noted that seismological data tends to be publicly accessible, especially through open-access repositories such as the Earthscope Data Services and the European Integrated Data Archive (EIDA). There is also a growing availability of hydrological data sets, such as those provided by the United States Geological Survey, the Hydro-Climatic Data Network (Lins, 2012), the National Water Information System (U.S. Geological Survey, 2020), NASA's Earth-Observing Giovanni system, and Copernicus Climate Change Service. Open seismic and hydrological data thus allow for both timely and long-term critical zone science.

7.2. *Developing unified physical models*

A critical challenge is the lack of a unified theoretical framework for integrating seismic observations with hydrological and geomorphological processes. Bridging the disciplines of continuum mechanics, granular physics, and soil science could lead to comprehensive models that capture the coupled effects of environmental influences. For instance, some studies have focused on nonlinear elasticity as a linear superposition of dilatational strains (e.g., Donaldson et al., 2019) or extensional strains (Okubo et al., 2024), or directly modeling $\mathrm{d}v/v$ terms (e.g., Sun et al., 2025), while others have focused on induced stresses (e.g., Fokker et al., 2021), and others use petrophysical models to estimate P and S wavespeed with water content (Solazzi et al., 2021; Z. Shen et al., 2024; Sobolevskaia et al., 2024).

An additional challenge is to separate elastic and poroelastic effects: seismic wavespeeds decrease in unconfined aquifers with increasing saturated but increase in confined aquifers due to the increased hydrological load (Delouche and Stehly, 2023). Furthermore, the coupling of thermoelastic stresses with hydrological processes is likely to play a role, given the large thermoelastic stresses in the critical zone (Sens-Schönfelder and Eulenfeld, 2019; Oakley et al., 2021; Sun et al., 2025). Collaborative efforts among seismologists, soil scientists, and hydrologists will be key to developing a unified physical model.

7.3. *Standardizing data processing*

Drawing unified models from the diverse literature on ambient noise monitoring for hydrological work is challenged by the individualized data processing scheme. Processing strategies for seismic data are currently study-specific, limiting the generalization and reproducibility of findings. Each study has a given sensor configuration, seismic frequency of interest (e.g., depth sensitivity), and lapse time in the coda (e.g., different wave types and spatial sensitivities for early vs. late coda), yielding a large variability in the proportionality between $\mathrm{d}v/v$ and groundwater levels (see Figure 5). Efforts to standardize preprocessing workflows, combined with the adoption of automated feature extraction and machine learning techniques (e.g., recent examples to predict river discharge or soil saturation directly from ambient noise Abi Nader et al. (2023) and Cunha Teixeira et al. (2025)), can accelerate the identification of hydrological signatures in seismic data. These advancements will also facilitate the development of transferable methodologies for broader applications in CZ science.

8. Conclusion

This review highlights the emerging role of ambient field seismology in bridging hydrological and geophysical sciences for monitoring the Critical Zone (CZ). Advances in ambient noise interferometry, coda wave analysis, and time-lapse tomography have demonstrated that near-surface seismic velocity and attenuation variations are intimately linked to changes in water saturation, pore pressure, and effective stress.

The range of applications covered in this review, from groundwater monitoring, vadose zone dynamics, slope stability, to seismic hazard assessment, may appear distinct, yet they reflect shared physical mechanisms: water-driven changes in subsurface stress and mechanical properties. Recognizing this, we advocate for a unified conceptual framework in which hydrological processes and geohazards are understood as coupled systems responding to climatatic and tectonic forcings.

Seismic velocity changes do not always behave uniformly with increasing water content: while pore pressure increases in saturated media typically reduce velocity, partial saturation and capillary effects in the vadose zone may increase soil stiffness and seismic speeds. These contrasting effects underscore the importance of site-specific rock physics, soil structure, and frequency-dependent wave sensitivity. The interpretation of seismic observables, whether $\mathrm{d}v/v$ or Q, must account for these regimes.

Across applications, the magnitude and timescale of seismic responses vary widely from sub-percent $\mathrm{d}v/v$ changes over hundreds of meters and tens of years in deep aquifers to rapid, multi-percent $\mathrm{d}v/v$ changes in shallow landslides. While the range of aforementioned spatial and temporal scales underscore the versatility of ambient noise monitoring, there is a need for standardized sensitivity metrics and frameworks to compare observations across hydrogeologic settings.

Fully realizing the potential of ambient field seismology will require transdisciplinary collaboration. Integrating seismic observations with hydrological modeling, soil physics, geotechnical engineering, remote sensing, and climate science is essential to build interpretable, scalable, and actionable monitoring systems. Beyond collaboration, this integration demands co-development of research questions, shared instrumentation strategies, and open data standards across traditionally siloed disciplines.

To translate these insights into practice, we outlined in Section 7 a set of specific future directions: from multi-sensor data fusion and physically informed modeling to standardization and reproducibility efforts. Together, these strategies can help realize the promise of passive seismic methods for understanding and forecasting critical zone dynamics in a changing world.

Table 1. Literature review of studies that have measured $\mathrm{d}v/v$ and compared with groundwater levels

Region	Wave type	Network	Freq (Hz)	ΔGWL (m)	Hydro estimate method	$\mathrm{d}v/v$ (%)	Reference
Southern CA, USA	Coda	Array	0.2–2	16	Well	0.10	Mao, Lecointre, et al. (2022)
CA, USA	Coda	Single	4–8	6	Rainfall	1.15	Clements and Denolle (2023)
San Gabriel, CA	Coda	Array	2–5	25	Well	0.15	Clements and Denolle (2018)
New Zealand	Coda	Small array	6–8	2	Piezo, seismometers	2.00	Voisin, Garambois, et al. (2016)
Lyon, France	Coda	Small Array	2–5	2	Piezo	2.50	Gaubert-Bastide et al. (2022)
Lyon, France	Coda	Small array	3–20	3	Piezo	2.50	Voisin, Guzmán, et al. (2017)
Ketzin, Germany	Coda	Array	1.4–3	0.6	Well	0.60	Gassenmeier et al. (2014)
Texas, USA	Coda	Single	0.01–8	25	Well	2.00	Kim and Lekic (2019)
Germany	Coda	Array	0.1–0.8	0.1	Well, water balance	0.01	Lecocq et al. (2017) (*)
Malta	Coda	Single	3–10	0.5	Well, rainfall	1.00	Laudi et al. (2023)
CA, USA	Coda	Small array	4–15	1.5	River gage	2.50	Rodríguez Tribaldos and Ajo-Franklin (2021)
Australia	Coda	Small array	20		0.3	2.00	Olivier et al. (2017)
Kyushu, Japan	Coda	Array	0.1–0.39	0.01	Rainfall	0.02	Q.-Y. Wang, Brenguier, et al. (2017) (*)
OK, USA	Coda	Array	0.1–1	0.15	GRACE	0.02	Zhang et al. (2023) (***)
Greece	Late coda	Single	0.3–1	2–5	Wells	0.03	Delouche and Stehly (2023)
Italy	Coda	Array	0.1–0.9	100	Geodetic inversion	0.10	Almagro Vidal et al. (2021)(**)
Germany	Late coda	Small array	1.5–3	0.4	Well	0.20	Gassenmeier et al. (2014)
Lyon, FR	Surface waves	Small array	3–40	2.5	Piezo and wells	1.50	Garambois et al. (2019)
Mojave, CA	Coda	Array	0.1–2	12	Well	0.10	Tsai (2011) and Meier et al. (2010)
Taiwan	Coda	Single	0.1–0.9	7	Well	0.40	Feng, Huang, Hsu, et al. (2021)

Regions, waves used, array configuration, sensor configuration, frequency band of measurements, groundwater level change ΔGWL (m), $\mathrm{d}v/v$(%) values reported, and references. The "rainfall" method refers to diffusion, either through poroelastic or baseflow models, of rainfall data. "single" refers to single station measurements, "small array" refers to arrays of geophones with less than 1 km in aperture, and "array" refers to regional seismic networks with inter-station spacing of about 10 km. (*) Converted from the hydraulic pressure $\mathrm{d}H = p/g\rho$, where $g = 9.81$, $\rho = 1000$ kg/m^3. (**) GWL is computed for 1000 km^2 basin. (***) Zhang et al. (2023) finds the following relation: $\mathrm{d}v/v = -1.68 \times 10^{-3}\Delta\mathrm{GWL} - 9.61 \times 10^{-3}$.

Acknowledgments

This research was partially funded by the David and Lucile Packard Foundation (MD). This manuscript has been co-authored by LV with number LA-UR-25-20095 by Triad National Security, LLC, under contract with the U.S. Department of Energy (no. 89233218CNA000001). LV was partially supported by the Los Alamos National Laboratory Center for Space and Earth Science Chick Keller Fellowship. TC was partially supported by a USGS Mendenhall fellowship. The authors thank the broader commu-

nity that has contributed to the discussion with MD about this review, namely Kuan-Fu Feng, Shujuan Mao, Stéphane Garambois, and Christophe Voisin. The authors thank two anonymous reviewers and Stephanie James for reviews that improved the manuscript. Much of the open-access data presented in the publications are hosted by the Earthscope Consortium Data Services through the National Science Foundation's Seismological Facility for the Advancement of Geoscience (SAGE) Award under Cooperative Agreement EAR-1724509. In European literature, EIDA is the European Integrated Data Archive infrastructure within ORFEUS to provide access to seismic waveform data in European archives.

Declaration of interests

The authors do not work for, advise, own shares in, or receive funds from any organization that could benefit from this article, and have declared no affiliations other than their research organizations.

Appendix

We summarize the values of $\mathrm{d}v/v$ and groundwater changes published in the literature in Table 1. The readers will find Python scripts to reproduce Figure 5 on https://github.com/Denolle-Lab/dvv-hydro-CompGeo-review-2024.

References

Abi Nader, A., J. Albaric, M. Steinmann, et al., "Machine learning prediction of groundwater heights from passive seismic wavefield", *Geophys. J. Int.* **234** (2023), no. 3, pp. 1807–1818.

Abrahamson, N. A. and R. R. Youngs, "A stable algorithm for regression analyses using the random effects model", *Bull. Seismol. Soc. Am.* **82** (1992), pp. 505–510.

Ajo-Franklin, J. B., S. Dou, T. Daley, et al., "Time-lapse surface wave monitoring of permafrost thaw using distributed acoustic sensing and a permanent automated seismic source", in *2017 SEG International Exposition and Annual Meeting*, SEG, 2017.

Aki, K., "Space and time spectra of stationary stochastic waves, with special reference to microtremors", *Bull. Earthquake Res. Inst.* **35** (1957), pp. 415–456.

Albaric, J., D. Kühn, M. Ohrnberger, N. Langet, D. Harris, U. Polom, I. Lecomte and G. Hillers, "Seismic monitoring of permafrost in Svalbard, Arctic Norway", *Seismol. Soc. Am.* **92** (2021), no. 5, pp. 2891–2904.

Almagro Vidal, C., L. Zaccarelli, F. Pintori, P. L. Bragato and E. Serpelloni, "Hydrological effects on seismic-noise monitoring in Karstic Media", *Geophys. Res. Lett.* **48** (2021), no. 15, article no. e2021GL093191.

Amalokwu, K., A. I. Best, J. Sothcott, M. Chapman, T. Minshull and X.-Y. Li, "Water saturation effects on elastic wave attenuation in porous rocks with aligned fractures", *Geophys. J. Int.* **197** (2014), no. 2, pp. 943–947.

Andajani, R. D., T. Tsuji, R. Snieder and T. Ikeda, "Spatial and temporal influence of rainfall on crustal pore pressure based on seismic velocity monitoring", *Earth Planet. Space* **72** (2020), pp. 1–17.

Anderson, R. S., S. P. Anderson and G. E. Tucker, "Rock damage and regolith transport by frost: an example of climate modulation of the geomorphology of the critical zone", *Earth Surf. Process. Landf.* **38** (2013), no. 3, pp. 299–316.

Andrews, D. J., "Objective determination of source parameters and similarity of earthquakes of different size", *Earthquake Source Mech.* **37** (1986), pp. 259–267.

Angelopoulos, M., T. Ryberg, C. F. Rasmussen, C. Haberland, B. Juhls, S. Dallimore, J. Boike and P. P. Overduin, "Passive seismology: lightweight and rapid detection of Arctic subsea and sub-aquatic permafrost", *J. Geophys. Res.: Earth Surf.* **129** (2024), no. 9, article no. e2023JF007290.

Aoi, S., T. Kunugi and H. Fujiwara, "Strong-motion seismograph network operated by NIED: K-NET and KiK-net", *J. Jpn. Assoc. Earthq. Eng.* **4** (2004), no. 3, pp. 65–74.

Babaeian, E., M. Sadeghi, S. B. Jones, C. Montzka, H. Vereecken and M. Tuller, "Ground, proximal, and satellite remote sensing of soil moisture", *Rev. Geophys.* **57** (2019), no. 2, pp. 530–616.

Baig, A. M., M. Campillo and F. Brenguier, "Denoising seismic noise cross correlations", *J. Geophys. Res.: Solid Earth* **114** (2009), no. B8, article no. B08310.

Barajas, A., L. Margerin and M. Campillo, "Coupled body and surface wave sensitivity kernels for coda-wave interferometry in a three-dimensional scalar scattering medium", *Geophys. J. Int.* **230** (2022), no. 2, pp. 1013–1029.

Barajas, A., P. Poli, N. D'Agostino, L. Margerin and M. Campillo, "Separation of poroelastic and elastic processes of an aquifer from tectonic phenomena using geodetic, seismic, and meteorological data in the Pollino Region, Italy", *Geochem. Geophys. Geosyst.* **22** (2021), no. 11, article no. e2021GC009742.

Befus, K. M., A. F. Sheehan, M. Leopold, S. P. Anderson and R. S. Anderson, "Seismic constraints on critical zone architecture, boulder creek watershed, front range, Colorado", *Vadose Zone J.* **10** (2011), no. 3, pp. 915–927.

Behm, M., F. Cheng, A. Patterson and G. S. Soreghan, "Passive processing of active nodal seismic data: estimation of V_P/V_S ratios to characterize structure and hydrology of an alpine valley infill", *Solid Earth* **10** (2019), no. 4, pp. 1337–1354.

Beresnev, I. A. and K.-L. Wen, "Nonlinear soil response–a reality?", *Bull. Seismol. Soc. Am.* **86** (1996), pp. 1964–1978.

Biskaborn, B. K., S. L. Smith, J. Noetzli, et al., "Permafrost is warming at a global scale", *Nat. Commun.* **10** (2019), no. 1, article no. 264.

Bonilla, L. F. and Y. Ben-Zion, "Detailed space–time variations of the seismic response of the shallow crust to small earthquakes from analysis of dense array data", *Geophys. J. Int.* **225** (2020), no. 1, pp. 298–310.

Bonilla, L. F., P. Guéguen and Y. Ben-Zion, "Monitoring coseismic temporal changes of shallow material during strong ground motion with interferometry and autocorrelation", *Bull. Seismol. Soc. Am.* **109** (2019), no. 1, pp. 187–198.

Boore, D. M., "Determining generic velocity and density models for crustal amplification calculations, with an update of the Boore and Joyner (1997) generic site amplification for", *Bull. Seismol. Soc. Am.* **106** (2016), no. 1, pp. 313–317.

Borcherdt, R. D., "Effects of local geology on ground motion near San Francisco Bay", *Bull. Seismol. Soc. Am.* **60** (1970), pp. 29–61.

Borgeat, X., F. Glueer, M. Häusler, M. Hobiger and D. Fäh, "On the variability of the site-response parameters of the active rock slope in Brienz/Brinzauls (Switzerland)", *Geophys. J. Int.* **240** (2024), no. 1, pp. 779–790.

Borgeat, X., F. Glueer, M. Häusler, M. Hobiger and D. Fäh, "On the variability of the site-response parameters of the active rock slope in Brienz/Brinzauls (Switzerland)", *Geophys. J. Int.* **240** (2025), no. 1, pp. 779–790.

Brantley, S. L., W. H. McDowell, W. E. Dietrich, et al., "Designing a network of critical zone observatories to explore the living skin of the terrestrial Earth", *Earth Surf. Dyn.* **5** (2017), no. 4, pp. 841–860.

Brenguier, F., M. Campillo, C. Hadziioannou, N. M. Shapiro, R. M. Nadeau and E. Larose, "Postseismic relaxation along the San Andreas Fault at Parkfield from continuous seismological observations", *Science* **321** (2008), no. 5895, pp. 1478–1481.

Brenguier, F., R. Courbis, A. Mordret, et al., "Noise-based ballistic wave passive seismic monitoring. Part 1: body waves", *Geophys. J. Int.* **221** (2020), no. 1, pp. 683–691.

Brenguier, F., N. M. Shapiro, M. Campillo, V. Ferrazzini, Z. Duputel, O. Coutant and A. Nercessian, "Towards forecasting volcanic eruptions using seismic noise", *Nat. Geosci.* **1** (2008), no. 2, pp. 126–130.

Burbey, T. J., "Stress–strain analyses for aquifer-system characterization", *Groundwater* **39** (2001), no. 1, pp. 128–136.

Butler, D. K., *Near-surface Geophysics*, Society of Exploration Geophysicists, 2005.

Cabrera-Pérez, I., L. D'Auria, J. Soubestre, et al., "Spatio-temporal velocity variations observed during the pre-eruptive episode of La Palma 2021 eruption inferred from ambient noise interferometry", *Sci. Rep.* **13** (2023), no. 1, article no. 12039.

Campillo, M. and A. Paul, "Long-range correlations in the diffuse seismic coda", *Science* **299** (2003), no. 5606, pp. 547–549.

Cannata, A., F. Cannavò, P. Montalto, M. Ercoli, P. Mancinelli, C. Pauselli and G. Leto, "Monitoring crustal changes at volcanoes by seismic noise interferometry: Mt. Etna case of study", *J. Volcanol. Geotherm. Res.* **337** (2017), pp. 165–174.

Chandra, J., P. Guéguen, J. H. Steidl and L. F. Bonilla, "In situ assessment of the g–γ curve for characterizing the nonlinear response of soil: application to the Garner Valley downhole array and the wildlife liquefaction array", *Bull. Seismol. Soc. Am.* **105** (2015), no. 2A, pp. 993–1010.

Chaney, N. W., J. K. Roundy, J. E. Herrera-Estrada and E. F. Wood, "High-resolution modeling of the spatial heterogeneity of soil moisture: applications in network design", *Water Resour. Res.* **51** (2015), no. 1, pp. 619–638.

Chapman, S., J. V. M. Borgomano, B. Quintal, S. M. Benson and J. Fortin, "Seismic wave attenuation and dispersion due to partial fluid saturation: direct measurements and numerical simulations based on X-Ray CT", *J. Geophys. Res.: Solid Earth* **126** (2021), no. 4, article no. e2021JB021643.

Cheng, F., N. J. Lindsey, V. Sobolevskaia, et al., "Watching the cryosphere thaw: seismic monitoring of permafrost degradation using distributed acoustic sensing during a controlled heating experiment", *Geophys. Res. Lett.* **49** (2022), no. 10, article no. e2021GL097195.

Clarke, D., L. Zaccarelli, N. M. Shapiro and F. Brenguier, "Assessment of resolution and accuracy of the moving window cross spectral technique for monitoring crustal temporal variations using ambient seismic noise", *Geophys. J. Int.* **186** (2011), no. 2, pp. 867–882.

Clements, T. and M. A. Denolle, "Tracking groundwater levels using the ambient seismic field", *Geophys. Res. Lett.* **45** (2018), no. 13, pp. 6459–6465.

Clements, T. and M. A. Denolle, "The seismic signature of california's earthquakes, droughts, and floods", *J. Geophys. Res.: Solid Earth* **128** (2023), no. 1, article no. e2022JB025553.

Collins, A. L., K. E. Allstadt and D. M. Staley, *Using the horizontal-to-vertical spectral ratio method to estimate thickness of the Barry Arm landslide, Prince William Sound, Alaska*, Technical Report, US Geological Survey, 2024.

Colombero, C., L. Baillet, C. Comina, D. Jongmans, E. Larose, J. Valentin and S. Vinciguerra, "Integration of ambient seismic noise monitoring, displacement and meteorological measurements to infer the temperature-controlled long-term evolution of a complex prone-to-fall cliff", *Geophys. J. Int.* **213** (2018), no. 3, pp. 1876–1897.

Colombi, A., J. Chaput, F. Brenguier, G. Hillers, P. Roux and M. Campillo, "On the temporal stability of the coda of ambient noise correlations", *C. R. Géosci.* **346** (2014), no. 11–12, pp. 307–316.

Condon, L. E., S. Kollet, M. F. Bierkens, et al., "Global groundwater modeling and monitoring: Opportunities and challenges", *Water Resour. Res.* **57** (2021), no. 12, article no. e2020WR029500.

Cunha Teixeira, J., L. Bodet, A. Rivière, et al., "Neural machine translation of seismic ambient noise for soil nature and water saturation characterization", *Geophys. Res. Lett.* **52** (2025), no. 13, article no. e2025GL114852.

Dai, F. C., C. F. Lee and Y. Y. Ngai, "Landslide risk assessment and management: an overview", *Eng. Geol.* **64** (2002), no. 1, pp. 65–87.

Delouche, E. and L. Stehly, "Seasonal seismic velocity variations measured using seismic noise autocorrelations to monitor the dynamic of aquifers in Greece", *J. Geophys. Res.: Solid Earth* **128** (2023), no. 12, article no. e2023JB026759.

Díaz, J., "On the origin of the signals observed across the seismic spectrum", *Earth-Science Rev.* **161** (2016), pp. 224–232.

Diewald, F., M. Denolle, J. J. Timothy and C. Gehlen, "Impact of temperature and relative humidity variations on coda waves in concrete", *Sci. Rep.* **14** (2024), no. 1, article no. 18861.

Donaldson, C., T. Winder, C. Caudron and R. S. White, "Crustal seismic velocity responds to a magmatic intrusion and seasonal loading in Icelands Northern Volcanic Zone", *Sci. Adv.* **5** (2019), no. 11, article no. eaax6642.

Dong, Y. and N. Lu, "Dependencies of shear wave velocity and shear modulus of soil on saturation", *J. Eng. Mech.* **142** (2016), no. 11, article no. 04016083.

Dou, S., N. Lindsey, A. M. Wagner, et al., "Distributed acoustic sensing for seismic monitoring of the near surface: a traffic-

noise interferometry case study", *Sci. Rep.* **7** (2017), no. 1, article no. 11620.

Eppinger, B. J., W. S. Holbrook, Z. Liu, B. A. Flinchum and J. Tromp, "2d near-surface full-waveform tomography reveals bedrock controls on critical zone architecture", *Earth Space Sci.* **11** (2024), no. 2, article no. e2023EA003248.

Esfahani, R., F. Cotton and L. F. Bonilla, "Temporal variations of the in-situ nonlinear behaviour of shallow sediments during the 2016 Kumamoto Earthquake sequence", *Geophys. J. Int.* **238** (2024), no. 3, pp. 1626–1637.

Eulenfeld, T. and U. Wegler, "Measurement of intrinsic and scattering attenuation of shear waves in two sedimentary basins and comparison to crystalline sites in Germany", *Geophys. J. Int.* **205** (2016), no. 2, pp. 744–757.

Everett, M. E., *Near-surface Applied Geophysics*, Cambridge University Press: Cambridge, 2013.

Feng, K.-F., H.-H. Huang, Y.-J. Hsu and Y.-M. Wu, "Controls on seasonal variations of crustal seismic velocity in taiwan using single-station cross-component analysis of ambient noise interferometry", *J. Geophys. Res.: Solid Earth* **126** (2021), no. 11, article no. e2021JB022650.

Feng, K.-F., H.-H. Huang and Y.-M. Wu, "Detecting pre-eruptive magmatic processes of the 2018 eruption at Kilauea, Hawaii volcano with ambient noise interferometry", *Earth Planet. Space* **72** (2020), pp. 1–15.

Flinchum, B. A., D. Grana, B. J. Carr, N. Ravichandran, B. Eppinger and W. S. Holbrook, "Low V_p/V_s values as an indicator for fractures in the critical zone", *Geophys. Res. Lett.* **51** (2024), no. 2, article no. e2023GL105946.

Flinchum, B. A., W. S. Holbrook and B. J. Carr, "What do P-wave velocities tell us about the critical zone?", *Front. Water* **3** (2022), article no. 772185.

Fokker, E., E. Ruigrok, R. Hawkins and J. Trampert, "Physics-based relationship for pore pressure and vertical stress monitoring using seismic velocity variations", *Remote Sens.* **13** (2021), no. 14, article no. 2684.

Fores, B., C. Champollion, G. Mainsant, J. Albaric and A. Fort, "Monitoring saturation changes with ambient seismic noise and gravimetry in a karst environment", *Vadose Zone J.* **17** (2018), no. 1, article no. 170163.

Gaillardet, J., I. Braud, F. Hankard, et al., "OZCAR: the French network of critical zone observatories", *Vadose Zone J.* **17** (2018), no. 1, article no. 180067.

Garambois, S., C. Voisin, M. A. Romero Guzman, D. Brito, B. Guillier and A. Réfloch, "Analysis of ballistic waves in seismic noise monitoring of water table variations in a water field site: added value from numerical modelling to data understanding", *Geophys. J. Int.* **219** (2019), no. 3, pp. 1636–1647.

Gassenmeier, M., C. Sens-Schönfelder, M. Delatre and M. Korn, "Monitoring of environmental influences on seismic velocity at the geological storage site for CO_2 in Ketzin (Germany) with ambient seismic noise", *Geophys. J. Int.* **200** (2014), no. 1, pp. 524–533.

Gaubert-Bastide, T., S. Garambois, C. Bordes, C. Voisin, L. Oxarango, D. Brito and P. Roux, "High-resolution monitoring of controlled water table variations from dense seismic-noise acquisitions", *Water Resour. Res.* **58** (2022), no. 8, article no. e2021WR030680.

Gehman, C. L., D. L. Harry, W. E. Sanford, J. D. Stednick and N. A. Beckman, "Estimating specific yield and storage change in an unconfined aquifer using temporal gravity surveys", *Water Resour. Res.* **45** (2009), no. 4, article no. W00D21.

Giardino, J. R. and C. Houser, "Introduction to the critical zone", in *Developments in Earth Surface Processes*, Elsevier, 2015, pp. 1–13.

Gochenour, J. A., S. L. Bilek, H. B. Woo, A. J. Luhmann, R. Grapenthin and J. B. Martin, "Ambient seismic noise tomography within the Floridan Aquifer System, Santa Fe river-Sink Rise, Florida, US", *J. Geophys. Res.: Solid Earth* **129** (2024), no. 5, article no. e2023JB027644.

Goodall, J. L., J. S. Horsburgh, T. L. Whiteaker, D. R. Maidment and I. Zaslavsky, "A first approach to web services for the National Water Information System", *Environ. Model. Softw.* **23** (2008), no. 4, pp. 404–411.

Gradon, C., F. Brenguier, J. Stammeijer, et al., "Seismic velocity response to atmospheric pressure using time-lapse passive seismic interferometry", *Bull. Seismol. Soc. Am.* **111** (2021), no. 6, pp. 3451–3458.

Greco, R., P. Marino and T. A. Bogaard, "Recent advancements of landslide hydrology", *WIREs Water* **10** (2023), no. 6, article no. e1675.

Grobbe, N., A. Mordret, S. Barde-Cabusson, et al., "A multi-hydrogeophysical study of a watershed at Kaiwi coast (o'ahu, hawai'i), using seismic ambient noise surface wave tomography and self-potential data", *Water Resour. Res.* **57** (2021), no. 4, article no. e2020WR029057.

Guillemot, A., A. Helmstetter, E. Larose, L. Baillet, S. Garambois, R. Mayoraz and R. Delaloye, "Seismic monitoring in the Gugla rock glacier (Switzerland): ambient noise correlation, microseismicity and modelling", *Geophys. J. Int.* **221** (2020), no. 3, pp. 1719–1735.

Guillemot, A., A. van Herwijnen, E. Larose, S. Mayer and L. Baillet, "Effect of snowfall on changes in relative seismic velocity measured by ambient noise correlation", *Cryosphere* **15** (2021), no. 12, pp. 5805–5817.

Hadziioannou, C., E. Larose, A. Baig, P. Roux and M. Campillo, "Improving temporal resolution in ambient noise monitoring of seismic wave speed", *J. Geophys. Res.: Solid Earth* **116** (2011), no. B7, article no. B07304.

Hadziioannou, C., E. Larose, O. Coutant, P. Roux and M. Campillo, "Stability of monitoring weak changes in multiply scattering media with ambient noise correlation: laboratory experiments", *J. Acoust. Soc. Am.* **125** (2009), no. 6, pp. 3688–3695.

Händel, A., M. Pilz, L. C. Malatesta, D. Litwin and F. Cotton, "Detecting seasonal differences in high-frequency site response using $\kappa 0$", *Seismica* **4** (2025), no. 1, pp. 1–14.

Hartog, A. H., *An Introduction to Distributed Optical Fibre Sensors*, CRC press: Boca Raton, 2017.

Hassani, B. and G. M. Atkinson, "Site-effects model for central and Eastern North America based on peak frequency and average shearwave velocity", *Bull. Seismol. Soc. Am.* **108** (2017), no. 1, pp. 338–350.

Hasselmann, K., "A statistical analysis of the generation of microseisms", *Rev. Geophys.* **1** (1963), no. 2, pp. 177–210.

He, B., H. Zhu and D. Lumley, "Improving signal-to-noise ratios of ambient noise cross-correlation functions using local attributes", *Geophys. J. Int.* **238** (2024), no. 3, pp. 1470–1490.

Hertrich, M., "Imaging of groundwater with nuclear magnetic resonance", *Prog. Nucl. Magn. Reson. Spectrosc.* **53** (2008), no. 4, pp. 227–248.

Higueret, Q., Y. Sheng, A. Mordret, et al., "Body waves from train noise correlations: potential and limits for monitoring the San Jacinto Fault, CA", *Geophys. J. Int.* **240** (2024), no. 1, pp. 721–729.

Hirose, T., H. Nakahara and T. Nishimura, "A passive estimation method of scattering and intrinsic absorption parameters from envelopes of seismic ambient noise cross-correlation functions", *Geophys. Res. Lett.* **46** (2019), no. 7, pp. 3634–3642.

Hirose, T., H. Ueda and E. Fujita, "Scattering and intrinsic absorption parameters of Rayleigh waves at 18 active volcanoes in Japan inferred using seismic interferometry", *Bull. Volcanol.* **84** (2022), no. 3, article no. 34.

Hirose, T., Q.-Y. Wang, M. Campillo, H. Nakahara, L. Margerin, E. Larose and T. Nishimura, "Time-lapse imaging of seismic scattering property and velocity in the northeastern Japan", *Earth Planet. Sci. Lett.* **619** (2023), article no. 118321.

Hobiger, M., U. Wegler, K. Shiomi and H. Nakahara, "Single-station cross-correlation analysis of ambient seismic noise: application to stations in the surroundings of the 2008 Iwate-Miyagi Nairiku earthquake", *Geophys. J. Int.* **198** (2014), pp. 90–109.

Hobiger, M., U. Wegler, K. Shiomi and H. Nakahara, "Coseismic and post-seismic velocity changes detected by passive image interferometry: comparison of one great and five strong earthquakes in Japan", *Geophys. J. Int.* **205** (2016), pp. 1053–1073.

Holzer, T. L. and T. L. Youd, "Liquefaction, ground oscillation, and soil deformation at the Wildlife Array, California", *Bull. Seismol. Soc. Am.* **97** (2007), no. 3, pp. 961–976.

Hotovec-Ellis, A. J., J. Gomberg, J. E. Vidale and K. C. Creager, "A continuous record of intereruption velocity change at Mount St. Helens from coda wave interferometry", *J. Geophys. Res.: Solid Earth* **119** (2014), no. 3, pp. 2199–2214.

Hua, J., M. Wu, J. P. Mulholland, J. D. Neelin, V. C. Tsai and D. T. Trugman, "High-resolution precipitation monitoring with a dense seismic nodal array", *Sci. Rep.* **13** (2023), no. 1, article no. 11450.

Hudson, T. S., J. M. Kendall, J. D. Blundy, M. E. Pritchard, P. MacQueen, S. S. Wei, J. H. Gottsmann and S. Lapins, "Hydrothermal fluids and where to find them: using seismic attenuation and anisotropy to map fluids Beneath Uturuncu Volcano, Bolivia", *Geophys. Res. Lett.* **50** (2023), no. 5, article no. e2022GL100974.

Illien, L., C. Andermann, C. Sens-Schönfelder, K. L. Cook, K. P. Baidya, L. B. Adhikari and N. Hovius, "Subsurface moisture regulates Himalayan groundwater storage and discharge", *AGU Adv.* **2** (2021), no. 2, article no. e2021AV000398.

Illien, L., J. M. Turowski, C. Sens-Schönfelder, C. Berenfeld and N. Hovius, "Predictable recovery rates in near-surface materials after earthquake damage", *Nat. Commun.* **16** (2025), no. 1, article no. 1790.

Ishihara, K., *Soil Behaviour in Earthquake Geotechnics*, Oxford Engineering Science Series, Clarendon Press, 1996.

James, S. R., H. A. Knox, R. E. Abbott, M. P. Panning and E. J. Screaton, "Insights into permafrost and seasonal active-layer dynamics from ambient seismic noise monitoring", *J. Geophys. Res.: Earth Surf.* **124** (2019), no. 7, pp. 1798–1816.

James, S. R., H. A. Knox, R. E. Abbott and E. J. Screaton, "Improved moving window cross-spectral analysis for resolving large temporal seismic velocity changes in permafrost", *Geophys. Res. Lett.* **44** (2017), no. 9, pp. 4018–4026.

James, S. R., B. J. Minsley, J. W. McFarland, E. S. Euskirchen, C. W. Edgar and M. P. Waldrop, "The biophysical role of water and ice within permafrost nearing collapse: insights from novel geophysical observations", *J. Geophys. Res.: Earth Surf.* **126** (2021), no. 6, article no. e2021JF006104.

Jemberie, A. L. and C. A. Langston, "Site amplification, scattering, and intrinsic attenuation in the Mississippi Embayment from Coda Waves", *Bull. Seismol. Soc. Am.* **95** (2005), no. 5, pp. 1716–1730.

Kim, D. and V. Lekic, "Groundwater variations from autocorrelation and receiver functions", *Geophys. Res. Lett.* **46** (2019), no. 23, pp. 13722–13729.

Klotzsche, A., F. Jonard, M. C. Looms, J. van der Kruk and J. A. Huisman, "Measuring soil water content with ground penetrating radar: a decade of progress", *Vadose Zone J.* **17** (2018), no. 1, pp. 1–9.

Kneisel, C., C. Hauck, R. Fortier and B. Moorman, "Advances in geophysical methods for permafrost investigations", *Permafrost Periglac. Process.* **19** (2008), no. 2, pp. 157–178.

Knight, R. and R. Nolen-Hoeksema, "A laboratory study of the dependence of elastic wave velocities on pore scale fluid distribution", *Geophys. Res. Lett.* **17** (1990), no. 10, pp. 1529–1532.

Köhler, A. and C. Weidle, "Potentials and pitfalls of permafrost active layer monitoring using the HVSR method: a case study in Svalbard", *Earth Surf. Dyn.* **7** (2019), no. 1, pp. 1–16.

Kramer, R., Y. Lu and G. Bokelmann, "Interaction of air pressure and groundwater as main cause of sub-daily relative seismic velocity changes", *Geophys. Res. Lett.* **50** (2023), no. 7, article no. e2022GL101298.

Kramer, R., Y. Lu, Q.-Y. Wang, S. Serafin, A. Ceppi and G. Bokelmann, "Identifying large vulnerable water reservoirs using passive seismic monitoring", *Earth Planet. Sci. Lett.* **653** (2025), article no. 119223.

Kula, D., D. Olszewska, W. Dobiński and M. Glazer, "Horizontal-to-vertical spectral ratio variability in the presence of permafrost", *Geophys. J. Int.* **214** (2018), no. 1, pp. 219–231.

Kuster, G. T. and M. N. Toksöz, "Velocity and attenuation of seismic waves in two-phase media: Part I. Theoretical formulations", *Geophysics* **39** (1974), no. 5, pp. 587–606.

Kwak, D. Y. and E. Seyhan, "Two-stage nonlinear site amplification modeling for Japan with VS30 and fundamental frequency dependency", *Earthq. Spectra* **36** (2020), no. 3, pp. 1359–1385.

Larose, E., S. Carrière, C. Voisin, et al., "Environmental seismology: What can we learn on earth surface processes with ambient noise?", *J. Appl. Geophys.* **116** (2015), pp. 62–74.

Laudi, L., M. R. Agius, P. Galea, S. D'Amico and M. Schimmel, "Monitoring of groundwater in a Limestone Island Aquifer using ambient seismic noise", *Water* **15** (2023), no. 14, article no. 2523. Online at https://www.mdpi.com/2073-4441/15/14/2523.

Lawrence, J. F., M. Denolle, K. J. Seats and G. A. Prieto, "A numeric evaluation of attenuation from ambient noise correlation functions", *J. Geophys. Res.: Solid Earth* **118** (2013), no. 12, pp. 6134–6145.

Le Breton, M., N. Bontemps, A. Guillemot, L. Baillet and E. Larose, "Landslide monitoring using seismic ambient noise correla-

tion: challenges and applications", *Earth-Sci. Rev.* **216** (2021), article no. 103518.

Lecocq, T., L. Longuevergne, H. A. Pedersen, F. Brenguier and K. Stammler, "Monitoring ground water storage at mesoscale using seismic noise: 30 years of continuous observation and thermo-elastic and hydrological modeling", *Sci. Rep.* **7** (2017), no. 1, pp. 1–16.

Lin, C.-R., S. von Specht, K.-F. Ma, M. Ohrnberger and F. Cotton, "Analysis of saturation effects of distributed acoustic sensing and detection on signal clipping for strong motions", *Geophys. J. Int.* **241** (2025), no. 2, pp. 971–985.

Lin, C.-Y., A. Miller, M. Waqar and L. T. Marston, "A database of groundwater wells in the United States", *Sci. Data* **11** (2024), no. 1, article no. 335.

Lin, Y.-P. and T. H. Jordan, "Elastic scattering dominates high-frequency seismic attenuation in Southern California", *Earth Planet. Sci. Lett.* **616** (2023), article no. 118227.

Lindner, F., J. Wassermann and H. Igel, "Seasonal freeze-thaw cycles and permafrost degradation on Mt. Zugspitze (German/Austrian Alps) revealed by single-station seismic monitoring", *Geophys. Res. Lett.* **48** (2021), no. 18, article no. e2021GL094659.

Lindsey, N. J., T. C. Dawe and J. B. Ajo-Franklin, "Illuminating seafloor faults and ocean dynamics with dark fiber distributed acoustic sensing", *Science* **366** (2019), no. 6469, pp. 1103–1107.

Linneman, D. C., C. E. Strickland and A. R. Mangel, "Compressional wave velocity and effective stress in unsaturated soil: potential application for monitoring moisture conditions in vadose zone sediments", *Vadose Zone J.* **20** (2021), no. 5, article no. e20143.

Lins, H. F., *USGS hydro-climatic data network 2009 (HCDN-2009)*, Technical Report, US Geological Survey, 2012.

Liu, H., J. Li, R. Hu, H. Meng and H. Lyu, "Quantitatively monitoring of seasonal frozen ground freeze–thaw cycle using ambient seismic noise data", *Seismol. Res. Lett.* **96** (2025), no. 1, pp. 282–293.

Liu, X., T. Zhu and J. Hayes, "Critical zone structure by elastic full waveform inversion of seismic refractions in a Sandstone Catchment, Central Pennsylvania, USA", *J. Geophys. Res.: Solid Earth* **127** (2022), no. 3, article no. e2021JB023321.

Liu, Z., C. Liang, C. Sens-Schönfelder, et al., "Monitoring crack opening via seismic velocity variation to assess that fatal effect of precipitation for landslide motion", *Earth Planet. Sci. Lett.* **644** (2024), article no. 118922.

Lobkis, O. I. and R. L. Weaver, "Coda-wave interferometry in finite solids: recovery of *P*-to-*S* conversion rates in an Elastodynamic Billiard", *Phys. Rev. Lett.* **90** (2003), no. 25, article no. 254302.

Lu, Y. and Y. Ben-Zion, "Regional seismic velocity changes following the 2019 Mw 7.1 Ridgecrest, California earthquake from autocorrelations and P/S converted waves", *Geophys. J. Int.* **228** (2021), no. 1, pp. 620–630.

Mainsant, G., E. Larose, C. Brönnimann, D. Jongmans, C. Michoud and M. Jaboyedoff, "Ambient seismic noise monitoring of a clay landslide: toward failure prediction", *J. Geophys. Res.: Earth Surf.* **117** (2012), no. F1, article no. F01030.

Makus, P., C. Sens-Schönfelder, L. Illien, T. R. Walter, A. Yates and F. Tilmann, "Deciphering the whisper of volcanoes: monitoring velocity changes at Kamchatka's Klyuchevskoy group with fluctuating noise fields", *J. Geophys. Res.: Solid Earth* **128** (2023), no. 4, article no. e2022JB025738.

Malagnini, L., "Velocity and attenuation structure of very shallow soils: evidence for a frequency-dependent Q", *Bull. Seismol. Soc. Am.* **86** (1996), no. 5, pp. 1471–1486.

Malagnini, L., T. Parsons, I. Munafò, S. Mancini, M. Segou and E. L. Geist, "Crustal permeability changes inferred from seismic attenuation: impacts on multi-mainshock sequences", *Front. Earth Sci.* **10** (2022), article no. 963689.

Mao, S., M. Campillo, R. D. van Der Hilst, F. Brenguier, L. Stehly and G. Hillers, "High temporal resolution monitoring of small variations in crustal strain by dense seismic arrays", *Geophys. Res. Lett.* **46** (2019), no. 1, pp. 128–137.

Mao, S., W. L. Ellsworth, Y. Zheng and G. C. Beroza, "Depth-dependent seismic sensing of groundwater recovery from the atmospheric-river storms of 2023", *Science* **387** (2025), no. 6735, pp. 758–763.

Mao, S., A. Lecointre, R. D. van der Hilst and M. Campillo, "Space–time monitoring of groundwater fluctuations with passive seismic interferometry", *Nat. Commun.* **13** (2022), no. 1, article no. 4643.

Mao, S., A. Mordret, M. Campillo, H. Fang and R. D. van der Hilst, "On the measurement of seismic traveltime changes in the time–frequency domain with wavelet cross-spectrum analysis", *Geophys. J. Int.* **221** (2019), no. 1, pp. 550–568.

Marc, O., C. Sens-Schönfelder, L. Illien, P. Meunier, M. Hobiger, K. Sawazaki, C. Rault and N. Hovius, "Toward using seismic intlierferometry to quantify landscape mechanical variations after earthquakes", *Bull. Seismol. Soc. Am.* **111** (2021), no. 3, pp. 1631–1649.

Margat, J. and J. Van der Gun, *Groundwater Around the World: a Geographic Synopsis*, CRC Press: London, 2013.

Margerin, L., A. Barajas and M. Campillo, "A scalar radiative transfer model including the coupling between surface and body waves", *Geophys. J. Int.* **219** (2019), no. 2, pp. 1092–1108.

Mavko, G. M. and A. Nur, "Wave attenuation in partially saturated rocks", *Geophysics* **44** (1979), no. 2, pp. 161–178.

Mayor, J., L. Margerin and M. Calvet, "Sensitivity of coda waves to spatial variations of absorption and scattering: radiative transfer theory and 2-D examples", *Geophys. J. Int.* **197** (2014), no. 2, pp. 1117–1137.

Meier, U., N. M. Shapiro and F. Brenguier, "Detecting seasonal variations in seismic velocities within Los Angeles basin from correlations of ambient seismic noise", *Geophys. J. Int.* **181** (2010), no. 2, pp. 985–996.

Mikesell, T. D., A. E. Malcolm, D. Yang and M. M. Haney, "A comparison of methods to estimate seismic phase delays: numerical examples for coda wave interferometry", *Geophys. J. Int.* **202** (2015), no. 1, pp. 347–360.

Molnar, S., J. F. Cassidy, S. Castellaro, et al., "Application of microtremor horizontal-to-vertical spectral ratio (MHVSR) analysis for site characterization: state of the art", *Sur. Geophys.* **39** (2018), pp. 613–631.

Mordret, A., R. Courbis, F. Brenguier, et al., "Noise-based ballistic wave passive seismic monitoring–Part 2: surface waves", *Geophys. J. Int.* **221** (2020), no. 1, pp. 692–705.

Murnaghan, F. D., "Finite deformations of an elastic solid", *Am. J. Math.* **59** (1937), no. 2, pp. 235–260.

Nagashima, F. and H. Kawase, "The relationship between V_s, V_p, density and depth based on PS-logging data at K-NET and KiK-net sites", *Geophys. J. Int.* **225** (2021), no. 3, pp. 1467–1491.

Nakahara, H., "Formulation of the spatial autocorrelation (SPAC) method in dissipative media", *Geophys. J. Int.* **190** (2012), no. 3, pp. 1777–1783.

Nakamura, Y., "A method for dynamic characteristics estimation of subsurface using microtremor on the ground surface", *Q. Rep. RTRI* **30** (1989), no. 1, pp. 25–33.

Nakata, N. and R. Snieder, "Near-surface weakening in Japan after the 2011 Tohoku-Oki earthquake", *Geophys. Res. Lett.* **38** (2011), article no. L17302.

Nur, A. and G. Simmons, "The effect of saturation on velocity in low porosity rocks", *Earth Planet. Sci. Lett.* **7** (1969), no. 2, pp. 183–193.

O'Connell, R. J. and B. Budiansky, "Seismic velocities in dry and saturated cracked solids", *J. Geophys. Res.* **79** (1974), no. 35, pp. 5412–5426.

Oakley, D. O., B. Forsythe, X. Gu, A. A. Nyblade and S. L. Brantley, "Seismic ambient noise analyses reveal changing temperature and water signals to 10s of meters depth in the critical zone", *J. Geophys. Res.: Earth Surf.* **126** (2021), no. 2, article no. e2020JF005823.

Obermann, A., B. Froment, M. Campillo, E. Larose, T. Planès, B. Valette, J. H. Chen and Q. Y. Liu, "Seismic noise correlations to image structural and mechanical changes associated with the Mw 7.9 2008 Wenchuan earthquake", *J. Geophys. Res.: Solid Earth* **119** (2014), no. 4, pp. 3155–3168.

Obermann, A., T. Planès, C. Hadziioannou and M. Campillo, "Lapse-time-dependent coda-wave depth sensitivity to local velocity perturbations in 3-D heterogeneous elastic media", *Geophys. J. Int.* **207** (2016), no. 1, pp. 59–66.

Obermann, A., T. Planès, E. Larose and M. Campillo, "Imaging preeruptive and coeruptive structural and mechanical changes of a volcano with ambient seismic noise", *J. Geophys. Res.: Solid Earth* **118** (2013), no. 12, pp. 6285–6294.

Obermann, A., T. Planès, E. Larose and M. Campillo, "4-D Imaging of subsurface changes with coda waves: numerical studies of 3-D combined sensitivity kernels and applications to the M_{w} 7.9, 2008 Wenchuan earthquake", *Pure Appl. Geophys.* **176** (2019), pp. 1243–1254.

Okay, H. B. and A. A. Özacar, "A novel VS30 prediction strategy taking fluid saturation into account and a new VS30 model of Türkiye", *Bull. Seismol. Soc. Am.* **114** (2023), no. 2, pp. 1048–1065.

Okubo, K., B. G. Delbridge and M. A. Denolle, "Monitoring velocity change over 20 years at Parkfield", *J. Geophys. Res.: Solid Earth* **129** (2024), no. 4, article no. e2023JB028084.

Olivier, G., F. Brenguier, T. de Wit and R. Lynch, "Monitoring the stability of tailings dam walls with ambient seismic noise", *Lead. Edge* **36** (2017), no. 4, 350a1–350a6.

Ostrovsky, L. A. and P. A. Johnson, "Dynamic nonlinear elasticity in geomaterials", *Riv. Nuovo Cim.* **24** (2001), no. 7, pp. 1–46.

Ouellet, S. M., J. Dettmer, G. Olivier, T. DeWit and M. Lato, "Advanced monitoring of tailings dam performance using seismic noise and stress models", *Commun. Earth Environ.* **3** (2022), no. 1, article no. 301.

Overduin, P. P., C. Haberland, T. Ryberg, F. Kneier, T. Jacobi, M. N. Grigoriev and M. Ohrnberger, "Submarine permafrost depth from ambient seismic noise", *Geophys. Res. Lett.* **42** (2015), no. 18, pp. 7581–7588.

Pacheco, C. and R. Snieder, "Time-lapse travel time change of multiply scattered acoustic waves", *J. Acoust. Soc. Am.* **118** (2005), no. 3, pp. 1300–1310.

Paitz, P., P. Edme, D. Gräff, F. Walter, J. Doetsch, A. Chalari, C. Schmelzbach and A. Fichtner, "Empirical investigations of the instrument response for distributed acoustic sensing (DAS) across 17 Octaves", *Bull. Seismol. Soc. Am.* **111** (2020), no. 1, pp. 1–10.

Park, C. B., R. D. Miller and J. Xia, "Multichannel analysis of surface waves", *Geophysics* **64** (1999), no. 3, pp. 800–808.

Pinzon-Rincon, L., D. Nziengui Bâ, A. Mordret, O. Coutant and F. Brenguier, "Monitoring near surface seismic attenuation variations using train tremors", *Geophys. Res. Lett.* **52** (2025), no. 11, article no. e2024GL113935.

Planès, T., E. Larose, L. Margerin, V. Rossetto and C. Sens-Schönfelder, "Decorrelation and phase-shift of coda waves induced by local changes: multiple scattering approach and numerical validation", *Waves Random Complex Media* **24** (2014), no. 2, pp. 99–125.

Poupinet, G., W. L. Ellsworth and J. Frechet, "Monitoring velocity variations in the crust using earthquake doublets: an application to the Calaveras Fault, California", *J. Geophys. Res.: Solid Earth* **89** (1984), no. B7, pp. 5719–5731.

Prieto, G. A., J. F. Lawrence and G. C. Beroza, "Anelastic earth structure from the coherency of the ambient seismic field", *J. Geophys. Res.: Solid Earth* **114** (2009), no. B7, article no. B07303.

Qin, L., Y. Ben-Zion, L. F. Bonilla and J. H. Steidl, "Imaging and monitoring temporal changes of shallow seismic velocities at the Garner Valley Near Anza, California, following the M7.2 2010 El Mayor-Cucapah earthquake", *J. Geophys. Res. Solid Earth* **125** (2020), no. 1, article no. e2019JB018070.

Rivet, D., F. Brenguier and F. Cappa, "Improved detection of preeruptive seismic velocity drops at the Piton de La Fournaise volcano", *Geophys. Res. Lett.* **42** (2015), no. 15, pp. 6332–6339.

Rodríguez Tribaldos, V. and J. B. Ajo-Franklin, "Aquifer monitoring using ambient seismic noise recorded with distributed acoustic sensing (DAS) deployed on dark fiber", *J. Geophys. Res.: Solid Earth* **126** (2021), no. 4, pp. 1–20.

Roeloffs, E., "Poroelastic techniques in the study of earthquake-related hydrologic phenomena" (Dmowska, R. and B. Saltzman, eds.), Adv. Geophys., Elsevier, 1996, pp. 135–195.

Roeloffs, E. A., "Persistent water level changes in a well near Parkfield, California, due to local and distant earthquakes", *J. Geophys. Res.: Solid Earth* **103** (1998), no. B1, pp. 869–889.

Roumelioti, Z., F. Hollender and P. Guéguen, "Rainfall-induced variation of seismic waves velocity in soil and implications for soil response: what the ARGONET (Cephalonia, Greece) vertical array data reveal", *Bull. Seismol. Soc. Am.* **110** (2020), no. 2, pp. 441–451.

Sakaki, T., D. M. O'Carroll and T. H. Illangasekare, "Direct quantification of dynamic effects in capillary pressure for drainage–wetting cycles", *Vadose Zone J.* **9** (2010), no. 2, pp. 424–437.

Sato, H., M. C. Fehler and T. Maeda, *Seismic Wave Propagation and Scattering in the Heterogeneous Earth*, Berlin, Heidelberg, 2012.

Schulz, W. H., J. B. Smith, G. Wang, Y. Jiang and J. J. Roering, "Clayey landslide initiation and acceleration strongly modulated by

soil swelling", *Geophys. Res. Lett.* **45** (2018), no. 4, pp. 1888–1896.

Seats, K. J., J. F. Lawrence and G. A. Prieto, "Improved ambient noise correlation functions using Welch's method", *Geophys. J. Int.* **188** (2012), no. 2, pp. 513–523.

Sens-Schönfelder, C. and T. Eulenfeld, "Probing the in situ elastic nonlinearity of rocks with earth tides and seismic noise", *Phys. Rev. Lett.* **122** (2019), no. 13, article no. 138501.

Sens-Schönfelder, C. and U. Wegler, "Passive image interferemetry and seasonal variations of seismic velocities at Merapi Volcano, Indonesia", *Geophys. Res. Lett.* **33** (2006), no. 21, pp. 1–5.

Shapiro, N. M., M. Campillo, L. Stehly and M. H. Ritzwoller, "High-resolution surface-wave tomography from ambient seismic noise", *Science* **307** (2005), no. 5715, pp. 1615–1618.

Shen, J. and T. Zhu, "Constraining water dynamics through unsaturated and saturated zones using fiber-optic seismic sensing data", *Earth Planet. Sci. Lett.* **666** (2025), article no. 119507.

Shen, Z., Y. Yang, X. Fu, K. H. Adams, E. Biondi and Z. Zhan, "Fiber-optic seismic sensing of vadose zone soil moisture dynamics", *Nat. Commun.* **15** (2024), no. 1, article no. 6432.

Sheng, Y., A. Mordret, F. Brenguier, et al., "Tracking seismic velocity perturbations at ridgecrest using ballistic correlation functions", *Seismol. Res. Lett.* **95** (2024), no. 4, pp. 2452–2463.

Siemon, B., A. V. Christiansen and E. Auken, "A review of helicopter-borne electromagnetic methods for groundwater exploration", *Near Surf. Geophys.* **7** (2009), no. 5–6, pp. 629–646.

Silver, P. G., T. M. Daley, F. Niu and E. L. Majer, "Active source monitoring of cross-well seismic travel time for stress-induced changes", *Bull. Seismol. Soc. Am.* **97** (2007), no. 1B, pp. 281–293.

Smail, R. A., A. H. Pruitt, P. D. Mitchell and J. B. Colquhoun, "Cumulative deviation from moving mean precipitation as a proxy for groundwater level variation in Wisconsin", *J. Hydrol. X* **5** (2019), no. June, article no. 100045.

Snieder, R., "Coda wave interferometry and the equilibration of energy in elastic media", *Phys. Rev. E* **66** (2002), no. 4, article no. 046615.

Sobolevskaia, V., J. B. Ajo-Franklin, F. Cheng, S. Dou, N. J. Lindsey and A. Wagner, "Monitoring water level of a surficial aquifer using distributed acoustic sensing and ballistic surface waves", *Water Resour. Res.* **60** (2024), no. 8, article no. e2023WR036172.

Socco, L. V., S. Foti and D. Boiero, "Surface-wave analysis for building near-surface velocity models—established approaches and new perspectives", *Geophysics* **75** (2010), no. 5, 75A83–75A102.

Solazzi, S. G., L. Bodet, K. Holliger and D. Jougnot, "Surface-wave dispersion in partially saturated soils: the role of capillary forces", *J. Geophys. Res.: Solid Earth* **126** (2021), no. 12, article no. e2021JB022074.

Song, Y.-Y., J. P. Castagna, R. A. Black and R. W. Knapp, "Sensitivity of near-surface shear-wave velocity determination from Rayleigh and Love waves", in *SEG Technical Program Expanded Abstracts 1989*, Society of Exploration Geophysicists, 1989, pp. 509–512.

Steidl, J. and P. Hegarity, "Instrumented field sites and liquefaction monitoring in the United States", in *Proceedings of the 16th World Conference on Earthquake Engineering*, International Association for Earthquake Engineering: Tokyo, 2017.

Steinmann, R., C. Hadziioannou and E. Larose, "Effect of centimetric freezing of the near subsurface on Rayleigh and Love wave velocity in ambient seismic noise correlations", *Geophys. J. Int.* **224** (2021), no. 1, pp. 626–636.

Steinmann, R., L. Seydoux and M. Campillo, "AI-based unmixing of medium and source signatures from seismograms: ground freezing patterns", *Geophys. Res. Lett.* **49** (2022), no. 15, article no. e2022GL098854.

Su, S. L., D. N. Singh and M. S. Baghini, "A critical review of soil moisture measurement", *Measurement* **54** (2014), pp. 92–105.

Sun, H., F. Cheng, J. Xia, J. Guan, Z. Li and J. B. Ajo-Franklin, "Unveiling cryosphere dynamics by distributed acoustic sensing and data-driven hydro-thermo coupled simulation", *Geophys. Res. Lett.* **52** (2025), no. 2, article no. e2024GL111188.

Syed, T. H., J. S. Famiglietti, M. Rodell, J. Chen and C. R. Wilson, "Analysis of terrestrial water storage changes from GRACE and GLDAS", *Water Resour. Res.* **44** (2008), no. 2, article no. W02433.

Tacher, L., C. Bonnard, L. Laloui and A. Parriaux, "Modelling the behaviour of a large landslide with respect to hydrogeological and geomechanical parameter heterogeneity", *Landslides* **2** (2005), pp. 3–14.

Taira, Taki and F. Brenguier, "Response of hydrothermal system to stress transients at Lassen Volcanic Center, California, inferred from seismic interferometry with ambient noise", *Earth Planet. Space* **68** (2016), pp. 1–13.

Takano, T., F. Brenguier, M. Campillo, A. Peltier and T. Nishimura, "Noise-based passive ballistic wave seismic monitoring on an active volcano", *Geophys. J. Int.* **220** (2019), no. 1, pp. 501–507.

Takano, T. and K. Nishida, "Tidal response of seismic wave velocity at shallow crust in Japan", *Geophys. Res. Lett.* **50** (2023), no. 9, article no. e2023GL103011.

Talwani, P., L. Chen and K. Gahalaut, "Seismogenic permeability, k_s", *J. Geophys. Res.: Solid Earth* **112** (2007), no. 7, pp. 1–18.

Toksöz, M. N., C. H. Cheng and A. Timur, "Velocities of seismic waves in porous rocks", *Geophysics* **41** (1976), no. 4, pp. 621–645.

Tsai, V. C., "A model for seasonal changes in GPS positions and seismic wave speeds due to thermoelastic and hydrologic variations", *J. Geophys. Res.: Solid Earth* **116** (2011), no. 4, pp. 1–9.

U.S. Geological Survey, *USGS Water Data for the Nation: U.S. Geological Survey National Water Information System Database*, 2020. Online at https://doi.org/10.5066/F7P55KJN.

Uecker, R. K., B. A. Flinchum, W. S. Holbrook and B. J. Carr, "Mapping bedrock topography: a seismic refraction survey and landscape analysis in the Laramie Range, Wyoming", *Front. Water* **5** (2023), article no. 1057725.

van Laaten, M. and U. Wegler, "Nonlinear inversion for a multilayer seismic s-wave attenuation model using radiative transfer theory", *J. Geophys. Res.: Solid Earth* **129** (2024), no. 8, article no. e2023JB027989.

Vassallo, M., G. Cultrera, G. Di Giulio, F. Cara and G. Milana, "Peak frequency changes from HV spectral ratios in Central Italy: effects of strong motions and seasonality over 12 years of observations", *J. Geophys. Res.: Solid Earth* **127** (2022), no. 5, article no. e2021JB023848.

Viens, L., L. F. Bonilla, Z. J. Spica, K. Nishida, T. Yamada and M. Shinohara, "Nonlinear earthquake response of marine sediments with distributed acoustic sensing", *Geophys. Res. Lett.* **49** (2022), no. 21, article no. e2022GL100122.

Viens, L. and B. G. Delbridge, "Shallow soil response to a buried chemical explosion with geophones and distributed acoustic

sensing", *J. Geophys. Res.: Solid Earth* **129** (2024), no. 7, article no. e2023JB028416.

Viens, L., M. A. Denolle, N. Hirata and S. Nakagawa, "Complex near-surface rheology inferred from the response of greater Tokyo to strong ground motions", *J. Geophys. Res. Solid Earth* **123** (2018), pp. 5710–5729.

Viens, L. and C. Van Houtte, "Denoising ambient seismic field correlation functions with convolutional autoencoders", *Geophys. J. Int.* **220** (2019), no. 3, pp. 1521–1535.

Voisin, C., S. Garambois, C. Massey and R. Brossier, "Seismic noise monitoring of the water table in a deep-seated, slow-moving landslide", *Interpretation* **4** (2016), no. 3, SJ67–SJ76.

Voisin, C., M. A. R. Guzmán, A. Réfloch, M. Taruselli and S. Garambois, "Groundwater monitoring with passive seismic interferometry", *J. Water Res. Protect.* **9** (2017), no. 12, pp. 1414–1427.

Wald, D. J. and T. I. Allen, "Topographic slope as a proxy for seismic site conditions and amplification", *Bull. Seismol. Soc. Am.* **97** (2007), no. 5, pp. 1379–1395.

Wang, Q.-Y., F. Brenguier, M. Campillo, A. Lecointre, T. Takeda and Y. Aoki, "Seasonal crustal seismic velocity changes throughout Japan", *J. Geophys. Res.: Solid Earth* **122** (2017), no. 10, pp. 7987–8002.

Wang, Q.-Y. and H. Yao, "Monitoring of velocity changes based on seismic ambient noise: a brief review and perspective", *Earth Planet. Phys.* **4** (2020), no. 5, pp. 532–542.

Wang, Y., J. Schmittbuhl, J. Azzola, F. Mattern, D. Zigone, O. Lengliné, V. Magnenet and J. Vergne, "Modeling the impact of seasonal water table fluctuations on ambient noise interferometry using acousto-elastic effect", *Geophys. Res. Lett.* **51** (2024), no. 18, article no. e2024GL110239.

Weatherill, G. A., S. R. Kotha, F. Cotton and L. Danciu, "Innovations in ground motion characterization for the 2020 European seismic hazard model (ESHM2020)", in *7th World Conference on Earthquake Engineering, Sendai, Japan*, 2020.

Weber, S., D. Fäh, J. Beutel, J. Faillettaz, S. Gruber and A. Vieli, "Ambient seismic vibrations in steep bedrock permafrost used to infer variations of ice-fill in fractures", *Earth Planet. Sci. Lett.* **501** (2018), pp. 119–127.

Wegler, U. and C. Sens-Schönfelder, "Fault zone monitoring with passive image interferometry", *Geophys. J. Int.* **168** (2007), no. 3, pp. 1029–1033.

Winkler, K. W. and A. Nur, "Seismic attenuation: effects of pore fluids and frictional-sliding", *Geophysics* **47** (1982), no. 1, pp. 1–15.

Xie, F., E. Larose, Q. Wang and Y. Zhang, "In-situ monitoring of rock slope destabilization with ambient seismic noise interferometry in southwest China", *Eng. Geol.* **312** (2023), article no. 106922.

Yang, X., J. Bryan, K. Okubo, C. Jiang, T. Clements and M. A. Denolle, "Optimal stacking of noise cross-correlation functions", *Geophys. J. Int.* **232** (2023), no. 3, pp. 1600–1618.

Youd, T. L., H. A. Bartholomew and J. S. Proctor, *Geotechnical logs and data from permanently instrumented field sites: Garner valley downhole array (GVDA) and wildlife liquefaction array (WLA)*, 2004. NEES@ UCSB Internal Report, p. 1–53.

Yu, C., Q.-Y. Wang, J. Ma and H. Yao, "Subsurface evolution of the seasonally frozen ground on the northeastern Tibetan Plateau from a perspective of seismic interferometry", *Geophys. J. Int.* **241** (2025), no. 1, pp. 308–325.

Yu, E., A. Bhaskaran, S. Chen, Z. E. Ross, E. Hauksson and R. W. Clayton, "Southern California earthquake data now available in the AWS cloud", *Seismol. Res. Lett.* **92** (2021), no. 5, pp. 3238–3247.

Yuan, C., J. Bryan and M. Denolle, "Numerical comparison of time-, frequency- and wavelet-domain methods for coda wave interferometry", *Geophys. J. Int.* **226** (2021), no. 2, pp. 828–846.

Yukutake, Y., T. Ueno and K. Miyaoka, "Determination of temporal changes in seismic velocity caused by volcanic activity in and around Hakone volcano, central Japan, using ambient seismic noise records", *Prog. Earth Planet. Sci.* **3** (2016), pp. 1–14.

Zhang, S., B. Luo, Y. Ben-Zion, D. E. Lumley and H. Zhu, "Monitoring terrestrial water storage, drought and seasonal changes in Central Oklahoma With ambient seismic noise", *Geophys. Res. Lett.* **50** (2023), no. 17, article no. e2023GL103419.

Zhu, C., F. Cotton, H. Kawase and B. Bradley, "Separating broadband site response from single-station seismograms", *Geophys. J. Int.* **234** (2023), no. 3, pp. 2053–2065.

Zhu, C., F. Cotton, H. Kawase and K. Nakano, "How well can we predict earthquake site response so far? Machine learning vs physics-based modeling", *Earthq. Spectra* **39** (2023), no. 1, pp. 478–504.

Zhu, C., G. Weatherill, F. Cotton, M. Pilz, D. Y. Kwak and H. Kawase, "An open-source site database of strong-motion stations in Japan: K-NET and KiK-net (v1. 0.0)", *Earthq. Spectra* **37** (2021), no. 3, pp. 2126–2149.